Tectonic Evolution of the Arkaroola Basin: Implications for the development of the Adelaide Rift Complex

Rowan Hansberry

Supervisors: David Giles, Alan Collins

October 2011

Centre for Tectonics, Resources and Exploration
School of Earth and Environmental Sciences
University of Adelaide, South Australia
rowan.hansberry@student.adelaide.edu.au

ABSTRACT

The Neoproterozoic to Cambro-Ordovician sediments of the Adelaide Rift Complex (formerly Adelaide Geosyncline) have been the focus of extensive investigation. Despite this, comparatively little is known about the Earliest Adelaidean Callanna Group sediments, due to their sparse preservation in outcrop geology. Exposure of the Callanna Group, and structures related to early Cryogenian graben formation at Arkaroola, in the northern Flinders Ranges, provides a unique opportunity to unravel the local geometries of rift initiation. These rocks have been subjected to multiple intracontinental deformations, most notably the Delamerian Orogeny. Through detailed structural mapping and analysis it is possible to propose models of tectonic evolution for this area. Previous regional scale mapping of the northern Flinders Ranges has identified a disparity between the tectonic history of the Arkaroola Basin and broader northern Flinders Ranges. The nature of the rifting and orogenic evolution of the Arkaroola Basin is determined though analysis of field data, rock samples in thin section and EBSD analysis. Graben formation accommodated an initial period of clastic and evaporitic deposition, followed by rift-related basalt extrusion. This was followed by several phases of localised rifting and deposition, controlled by evolving fault geometries. Broad-scale orthogonal folding has folded an earlier composite fabric in conjunction with bedding. This initially planar fabric, most notable in the Woodnamoka Phyllite, formed during peak metamorphism of at least 500° C and approximately 3 kbars and is primarily attributed to burial beneath a thick pile of rift and sag phase sediments, coupled with a change in horizontal stresses. This is loosely constrained to post-rift cessation and before a previously indentified thermal pulse, *ca* 440 Ma. A set of NE-SW trending faults in the basin have been identified as En echelon stepovers of the Paralana Fault system, responsible for the formation of the pull-apart geometries. This system of faults details a strike-slip duplex, the reactivation of which, coupled with an anomalously high-heat producing basement, has controlled and localised deformation of the Arkaroola Basin.

Keywords: Adelaide, rift, Geosyncline, Willouran, Callanna, Paralana, duplex, Flinders, Arkaroola.

TABLE OF CONTENTS

1. INTRODUCTION

This paper presents a detailed investigation of the depositional and structural evolution of the earliest phase of the Adelaide Rift Complex (ARC) in the northern Flinders Ranges, South Australia. This was accomplished through detailed mapping of the lithologies and structures (coupled with analytical investigation) of the Arkaroola region, onlapping the south-western extent of the Mt. Painter Province (Figure 1).

The ARC has been the subject of extensive study since the early 1950s (Mawson & Sprigg 1950) and significant bodies of work have been published investigating the structural and sedimentary history of the ARC (Preiss 1987, Drexel *et al.* 1993, Powell *et al.* 1994, Priess 2000), as well as the timing and nature of the deformation which has shaped the modern day distribution of these rocks into the Flinders and Mount Lofty Ranges (Marshak & Flottmann 1996, Paul *et al.* 1999, Foden *et al.* 2006).

The ARC encompasses the Neoproterozoic to Cambro-Ordovcian sediments of the Adelaide Geosyncline (Preiss 1987, Priess 2000) and the Palaeo-Mesoproterozoic crystalline basement (Mildren & Sandiford 1995). Sedimentation in the Adelaidean system is inferred to have commenced *ca* 830 Ma (Powell *et al.* 1994) accommodating a Neoproterozoic rift succession until the *ca* 700 Ma break-up of the supercontinent Rodinia and accumulation of a passive margin wedge. The earliest phases of rifting are represented by the deposition of the basal Adelaidean, which was localised by partial graben formation and is sparsely preserved. Early rift structures and geometries are poorly defined; these structures are buried by subsequent sedimentation and reoriented by ensuing basement-involved deformation, localised along reactivated normal faults (Paul *et al.* 1999). The current understanding of rift geometries is based primarily on indirect or imprecise evidence, such as the orientation of the NW trending Gairdner Dyke Swarm or the modern distribution of sediments – defining a generally N to S trending rift margin. However, proposing the orientation of rifting from

structures like these may be presumptuous. Li *et al*. (2008) suggests that rifting and break-up of Rodinia occurred as a result of a mantle superplume, and as such, it is possible the Gairdner dykes may be part of a radial swarm and not indicative of regional extensional direction.

The area surrounding the Arkaroola Village in the northern Flinders Ranges (Figure 1b) preserves the earliest Adelaidean sediments of the Callanna Group. Previous workers (Sandiford *et al.* 1998, Paul *et al.* 1999, Elburg *et al.* 2003, Backe *et al.* 2010) have identified that the Paralana Fault played a prominent role in early rifting. Previous mapping, largely based on the original survey (Coats 1973) has identified similarly trending faults in the area, though little attempt has been made to infer the role that these may have played in early rift development.

2. GEOLOGICAL AND TECTONIC SETTING

2.1 Rodinia: Supercontinental Assembly and Break-up

The supercontinent Rodinia was formed during the period from 1300 to 900 Ma through worldwide orogenic events involving the collision or accretion of virtually all known continental blocks around the margin of Laurentia (Li *et al.* 1995, Li *et al.* 1999, Pisarevsky *et al.* 2003, Wang & Li 2003, Cawood 2005, Li *et al.* 2008). This Laurentia-centric model of assembly and break-up is widely accepted due to the Neoproterozoic passive margins flanking the Laurentian Block (Hoffman 1991). Rodinia existed for approximately 150 million years before a diachronous break-up (Lindsay *et al.* 1987). Several theories exist for the assembly of continental blocks within Rodinia, based on geological, geochronological and palaeomagmatic data which provide correlations across the now separated continental margins. Several publications (Li *et al.* 1995, Li *et al.* 1999, Li *et al.* 2008) have suggested that the South China Block was situated between Laurentia and Australia-East Antarctica in a "missing-link" model of Rodinian assembly.

Mantle avalanches combined with thermal insulation are proposed to have formed a mantle superswell beneath Rodinia 40-60 million years after its formation (Li *et al.* 2008). The plume head is interpreted to have been located beneath South China and resulted in continental doming (Wang *et al.* 2010) followed by widespread continental rifting and magmatism in four distinct episodes through the period 830-700 Ma (Powell *et al.* 1994, Priess 2000, Wang & Li 2003), which detail the polyphase break-up of Rodinia.

Wang *et al*. (2010) have proposed a geodynamic model for a mantle plume impinging on the continental lithosphere beneath the Yangtze (South China) Craton *ca* 830 Ma. This could have in part deflected to an existing weak zone in the lithosphere between the Yangtze and Australian Cratons, forming the Bikou-Hannan Rift. It has long been suggested that the Adelaide Geosyncline could

represent an aulacogen or failed-arm of a triple-junction rift (Burke & Dewey 1973, Preiss 1987). These systems are typical of continental break-up (Houseman 1990, 1991, Li *et al.* 1999, Wolfenden *et al.* 2004) and Wang *et al*. (2010) goes on to suggest that ARC and the Bikou-Hannan Rift formed such a triple-junction, with the ARC arm failing as the two continents separated. The remaining intracontinental filled graben preserves an impressive record of the process of continental break-up.

2.2 The Adelaide Rift Complex

The Palaeoproterozoic to Mesoproterozoic basement below the Adelaidean rift basins is markedly younger that most of the Gawler Craton. Preiss (2000) suggested a late Palaeoproterozoic pre cursor basin, which would likely have covered roughly the same area as the Neoproterozoic ARC. Sedimentation as well as volcanism occurred during the period 1750-1650 Ma, likely followed by an orogenic event *ca* 1600 Ma.

Deposition of the Adelaidean sediments is inferred to have begun *ca* 830 Ma in the Early Willouran. The “series” terms Willouran and Torrensian (followed by the Sturtian and Marinoan) were first used by Mawson & Sprigg (1950) in a chronostratigraphic sense, defining periods of the Neoproterozoic history of the Adelaidean system, independent of lithostratigraphic subdivision (Powell *et al.* 1994). This paper uses these terms in the same convention.

Several authors (Hilyard 1990, Powell *et al.* 1994, Wingate *et al.* 1998, Priess 2000) have interpreted that basal Adelaidean sedimentation took place in stable, intracratonic sag basins, with minor development of NW trending half-grabens and rift troughs. These were inferred (Hilyard 1990) to have formed along the crest of regional syn-magmatic doming associated with a mantle superplume

beneath the Rodinian supercontinent (Li *et al.* 1995, Li *et al.* 1999, Li *et al.* 2008). Preiss (2000) suggested a second phase of Willouran deposition *ca* 802 Ma producing narrow NW to NNW trending grabens, infilled with a mix of evaporitic clastics and carbonates. Hilyard (1990) and Crawford & Hilyard (1990) concluded that early Willouran deposition was overlain by subaerial eruption of tholeiitic plateau basalts (the Wooltana Volcanics and equivalents) originating from deep-seated faults during early rifting *ca* 827 Ma. This inference is based on the geochemically ascribed co-magmatic relationship between the Wooltana flood basalts and the doleritic Gairdner Dyke Swarm of the Gawler Craton (Figure 1a) – the intrusion of which is constrained by an 827±6 Ma SHRIMP U-Pb zircon age (Wingate *et al.* 1998). Though these eruptions occurred during extension and normal faulting, thick rift-valley successions and basal fan-type deposits are absent during volcanism and first occur stratigraphically above the volcanics. This is taken to indicate the rate of volcanism and subsidence was proportional, forming lava plateaus.

Torrensian time records a third phase of rifting characterised by N to S trending rift margins (Powell *et al.* 1994). The broader deposition of the Burra Group sediments indicates that the zone of crustal extension widened with the onset of Torrensian rifting. The Burra Group oversteps the Callanna with its terrestrial to shallow marine sediments overlapping the Willouran grabens and basement comprised rift shoulders (Preiss 1987, Priess 2000). Hilyard (1990) inferred that this period of major subsidence and graben formation was likely due to a combination of widely inferred regional extension, coupled with the evacuation of capacious magma chambers and isostatic adjustment.

2.3 Early Adelaidean Stratigraphy

The Adelaidean rift sediments were subdivided into lithostratigraphic units (Thompson *et al.* 1964) and whilst these have received numerous refinements (Preiss 1987, Drexel *et al.* 1993, Preiss *et al.* 1998) this classification is maintained today (Priess 2000). The subdivision proposed (Preiss 1982) is made up of the Warrina, Heysen and Moralana Supergroups. This paper is concerned with the Warrina Supergroup which comprises the early rift sequences of the Callanna and Burra Groups (Priess 2000).

2.3.1 THE CALLANNA GROUP

The Callanna Group incorporates the first sediments deposited in Willouran intracratonic sag-basins as well as the overlying Wooltana flood basalts and related volcanics. Stratigraphic relationships between these rocks and the overlying Burra Group sediments are poorly preserved and are most commonly seen as tectonic or diapiric contacts (Priess 2000). The basal Arkaroola Subgroup features quartzose and arkosic sediments, overlying and intertonguing carbonates and extensive flood basalts (Powell *et al.* 1994). These sequences show indications of evaporitic depositional environments with no regional palaeoslope or evidence to suggest marine inundation (Priess 2000). These earliest Adelaidean sequences outcrop in the northern Flinders Ranges where they have been locally metamorphosed to amphibolite facies. The basal siliclastics are represented by the mature to supermature (Priess 2000) Paralana Quartzite and the carbonates by marbles and calc-silicates of the Wywyana Formation. The Wooltana Volcanics overlie the Wywyana in the northern Flinders Ranges, forming the top of the Arkaroola Subgroup. They outcrop extensively as sub-aerial tholeiitic flood basalts (Wingate *et al.* 1998) and are variably altered with minor dolerite-gabbro intrusions (Wang *et al.* 2010).

2.3.2 THE BURRA GROUP

The Torrensian Burra Group is the oldest major succession of sediments widely preserved (and outcropped) in the ARC (Priess 2000), the broader deposition of which indicates a widening of the zone of rifting. The Burra Group is also subdivided and the base is represented by the intertonguing Emeroo and Wakefield Subgroups. At Arkaroola the Emeroo Subgroup consists of the basal, pebbly quartzite of the Humanity Seat Formation which intertongues with the Woodnamoka Phyllite to the west of the Paralana Fault (Preiss 1987), interpreted as an active rift structure bounding a deep graben. These two units are interpreted as laterally equivalent (Drexel *et al.* 1993). These units are overlain by the arkosic Blue Mine Conglomerate (Preiss 1987), followed by the dolomitic siltstones of the Opaminda Formation. The original regional survey (Coats 1973) incorporated all units below the Opaminda into the "Callanna Beds" but others (Forbes *et al.* 1981) included the Humanity Seat Formation, Woodnamoka Formation and Blue Mine Conglomerate within the lower Burra Group and this revision has been adopted by subsequent workers.

Overlying the early rift sediments are transgression-regression cycles of the Middle and Upper Burra Group, marking an episode of regional thermal subsidence (Paul *et al.* 1999). A passive margin wedge accumulated as Rodinia broke apart *ca* 700 Ma (Powell *et al.* 1994) and deposition continued in the Sturtian, before the passive margin was transformed into a convergence zone (Powell *et al.* 1994). Sedimentation in the ARC had terminated by the Cambro-Ordovician Delamerian Orogeny.

2.4 Regional Structure and Deformation

The ARC was deformed and metamorphosed by the Delamerian Orogeny, an episode of major crustal shortening *ca* 500 Ma (Marshak & Flottmann 1996, Foden *et al.* 2006). The northern Flinders Ranges is characterised by basement involved deformation, with both the Palaeo-Mesoproterozoic basement and the Neoproterozoic cover affected. The sedimentary package is now confined to an area of topographic elevation which makes up the Flinders and Mt. Lofty Ranges and this modern day landscape is a result of the reactivation of the fold belt during the Tertiary (Paul *et al.* 1999). The northern Flinders Ranges is characterised by large-scale open folding, verging to the south, often associated with pop-up geometries. Here the basement has been heavily involved in variably intense folding and contractional faulting (Priess 2000). Strain was concentrated along deep-rooted basement faults and sedimentary décollements played little role in accommodating slip (Paul *et al.* 1999). Basement structures which were active as extensional normal faults during the earlier rifting were reactivated as thrusts whilst transform faults perpendicular to rift margins reactivated with strike slip movement.

2.4.1 MAJOR STRUCTURES IN THE NORTHERN FLINDERS RANGES

The northern Flinders Ranges is bound by two major faults. The eastern margin of the region, where the Mt. Painter and Mt. Babbage Inliers are juxtaposed against the Curnamona Province, is marked by the Paralana Fault. The western limit, of the northern Flinders Ranges, is marked by the Norwest Fault. Paul *et al*. (1999) described both of these structures as having been important growth faults during the early rift-phase deposition, with depocentres located at times in the hangingwall side of each.

The Paralana fault is a steeply north-west dipping structure located to the east of the Arkaroola Village. Paul *et al*. (1999) concluded that the Paralana Fault exerted control on deposition during rifting; with largely sinistral strike slip movement as the structure acted as a transfer fault for extension. The reactivation of the Paralana Fault in the Delamerian comprises a conversely dextral transpressional regime in which both the Paralana and Norwest Faults, coupled with fault propagation folding in their hangingwalls, accommodated the bulk of shortening in the northern Flinders Ranges (Paul *et al.* 1999).

2.4.2 EXHUMATION OF THE MT. PAINTER INLIER

As stated, reactivation of the Delamerian Fold Belt in the Tertiary was responsible for the current topography and exhumation of basement inliers. Through restored cross sections Paul *et al*. (1999) illustrated that the reverse movement along the Paralana Fault as well as steeply south-east dipping basement faults in the Terrapinna Corridor (between the Mt. Painter and Mt. Babbage Inlier) exhumed the Mt. Painter, with pop-up style geometry.

2.4.3 DEFORMATION IN THE MT PAINTER AREA

Metamorphic conditions in the Adelaide Fold Belt were generally low grade, the northern Flinders Ranges reaching predominantly greenschist facies. Contrastingly, areas around the Mt. Painter Inlier reach amphibolite facies (Mildren & Sandiford 1995) with an estimated peak at 500-550°C attained at depths of only 10-12 km. In the Arkaroola area this high-temperature, low-pressure metamorphism has resulted in the alteration of pelitic sediments to biotite-andalusite-cordierite schists (Elburg *et al.* 2003). The variation in metamorphic grade predominantly increases with proximity to the Mt. Painter Inlier, and has been ascribed to high heat production in basement granites (McLaren *et al.* 2002, Elburg *et al.* 2003).

The Adelaidean units overlying the basement display a cleavage produced by Delamerian deformation, defined by an alignment of biotite. The andalusite and cordierite porphyroblasts found in the schists appear to have been syn- to late-tectonic, wrapped around and pervaded by this tectonic fabric (Elburg *et al.* 2003). Elburg *et al*. (2003) noted two minor crenulations in the more pelitic beds though, citing the complexity of structures in this region they were not correlated with a specific event. Widespread alteration, specifically of the Wooltana Volcanics and Wywyana Formation occurs extensively, often corresponding to faults and shear zones. Here these lithologies are comprehensively altered to an actinolite rock, completely lacking in fabric, indicating that alteration post-dates the Delamerian (Elburg *et al.* 2003).

Elburg *et al*. (2003) concluded that Delamerian deformation in Arkaroola resulted in ductile deformation which produced folding and associated cleavages in both the basement and cover. This was coupled with the formation of biotite-andalusite-cordierite schists from the prograde metamorphism of pelitic lithologies. Eventual uplift and cooling led to brittle deformation that was localised along faults.

3. FIELD RELATIONSHIPS

While various authors have postulated theories for the assembly, framework and eventual break-up of Rodinia, these suppositions and the processes involved are still a matter of debate. The character and geometries of the early history of the ARC are poorly constrained, with most inferences taken from indirect evidence. To assist in building an understanding of the early rift phases and the geometries involved, a field study was undertaken. A detailed geological map of the area was produced (Figure A), following on from the map adapted by Preiss (1987) from the original Coats & Blissett survey. This mapping identified and built upon the earlier descriptions of the Callanna and Burra Group lithologies, granitic basement and significant structures of the area north of the Arkaroola Village.

3.1 Lithologies

MT. NEILL GRANITIC BASEMENT

Forming the basement of the Adelaidean in the Arkaroola region is the Mt Neill Granite porphyry of the southernmost edge of the Mt. Painter Basement Complex. This rock is of granitic composition – predominantly quartz, K-feldspar, biotite and muscovite. The granite is typified by 3-8 mm blue quartz augen (Figure 2A) and large (up to 3 cm) K-feldspar augen.

PARALANA QUARTZITE

The Adelaidean basement is overlain by the Paralana Quartzite, this contact marking an erosional unconformity (Figure 2B). This unit is a well bedded, often massive, pink to grey-weathering orthoquartzite featuring interbeds of more argillaceous layers between thicker, pure quartzites. The lithology also features more arkosic layers of a poorly sorted, pink to grey and red-weathering meta-sandstone. This rock type has a gritty texture with a kaolitic-sericitic matrix between coarse arkosic

grains and features numerous sedimentary structures. A type location for the Paralana Quartzite and the underlying basement near Arkaroola Waterhole displays the unconformity overlain by a 6-10 m layer of massively bedded quartzite with minor, thin interbeds of finer sands and silts. The sequence typically fines into interbeds of argillaceous material and thickly bedded, pure quartzite. Conversely, the lower Callanna succession to the west of Mt. Oliphant commences with a poorly sorted, arkosic arenite. This unit is observed with minor, more quartzose interbeds for a thickness of approximately 50m before it grades into the more typical massive quartzite. Total sedimentary thickness for this unit is estimated at 100-350m with Preiss (1987) asserting a maximum thickness of 400m west of the Paralana Fault.

WYWYANA FORMATION

The Paralana Quartzite grades conformably into the overlying Wywyana Formation with an increasing calcic component through the transition. The Wywyana Formation is composed of actinolitic marbles, minor calc-silicate hornfels and meta-siltstones. Amphibole percentage (actinolite and tremolite) varies through the unit with some exposures consisting of massive, completely crystalline, actinolitic rubble. This rock type has an approximate composition of 70% actinolite, 20% biotite and 10% anhydrite/diopside/feldspar ± Fe-oxides/tremolite and is typically found in proximity to faults or lithological contacts with volcanics. These relationships display a gradational change from marbles to actinolite marbles to rubble nearing the structure; there is no discernable fabric in the actinolite rubble. Given the erratic nature of folding in this unit it is difficult to estimate a sedimentary thickness for this formation; however structural observations lead this author to infer a thickness of approximately 80-140m.

WOOLTANA VOLCANICS

The Wooltana Volcanics overly the Wywyana Formation conformably in an idealised stratigraphic column, though due to the nature of their extrusion they infrequently occur emplaced in the

Callanna Beds. This unit outcrops as fine to medium grained, grey-green to red-purple weathering, and often homogenous basalts. Variation in texture is however noted throughout the area with porphyroblastic, vesicular and amygdaloidal textures common. Calcium rich mineralogy is frequently observed in the abundance of secondary actinolite and epidote likely formed by metasomatism along fractures and other planar surfaces.

HUMANITY SEAT FORMATION

A depositional time-gap exists between the Wooltana Volcanics and the disconformably overlying Humanity Seat Formation due to the absence in this location of the Curdimurka Subgroup, which is inferred to exist between them stratigraphically. The Humanity Seat Formation is a medium grained, quartz rich meta-sandstone typified by minor interbeds of purple shales and extensive heavy mineral laminations and cross stratification. A maximum thickness for this unit is estimated at approximately 1.4 km to the west of the ECF.

Overlying the Humanity Seat Formation is a newly defined sedimentary breccia which has previous been classified as a breccia bed at the base of the Woodnamoka Phyllite and thought to represent a disconformity within the Emeroo Subgroup (Drexel *et al.* 1993). This unit is composed of diamictic clasts, 2-10 cm, predominantly of quartz, quartzite and volcanics as well as minor sediments and gneisses (Figure 2C). The matrix is a medium- to coarse-grained quartzose meta-sandstone. The similarities between the matrix (with abundant laminations and sedimentary structures) and the Humanity Seat Formation lead this author to ascribe this unit to the latter, rather than the Woodnamoka Phyllite. Like the Humanity Seat Formation it thins to the west, with both pinching out around the Arkaroola Pegmatite. The contact between this unit and the underlying Humanity Seat Formation, as well as the overlying Woodnamoka Phyllite is conformable and gradational.

WOODNAMOKA FORMATION

Overlying the Wywyana Phyllite in the west and the Arkaroola Creek Breccia Member in the east is the Woodnamoka Phyllite. Overlying the lower pelitic lithologies is a fine- to medium-grained, grey to red weathering and often micaceous arenite. This is interbedded with 5-10m packages of pelitic sediments, metamorphosed to biotite-andalusite schist. Within approximately 100m this unit grades into a medium to coarse grained, pink-orange to red weathering felspathic arenite which is termed the Oliphant Arkose Member (OAM). This unit is less micaceous and generally lower grade in appearance, preserving extensive cross-stratification and ripple casts. This unit forms a prominent ridge to the east of Mt. Oliphant, and is interpreted to be laterally extensive throughout the Woodnamoka at an approximate thickness of 100-120 m.

Overlying the OAM is another pelitic unit with well laminated siltstones metamorphosed to phyllites and interbedded with biotite-andalusite schists in 5-20 m packages. The phyllites shows thin laminations (1-2 mm) of very light material with larger (cm scale) packages of dark, heavy mineral rich silts.

The top of the Woodnamoka Formation exhibits a medium- to coarse-grained, gritty, red weathering arkosic unit, interbedded with sporadic finer sands and silts. Andalusite porphyroblasts appear throughout, frequently in laminar lenses. Unlike the lower sequences of the Woodnamoka these porphyroblasts are not limited to the schistose pelitic layers. This rock type forms a transitional sub-unit of the Woodnamoka in both a sedimentary and a metamorphic sense. Clasts associated with the Blue Mine Conglomerate can be found towards the top of the transitional package.

BLUE MINE CONGLOMERATE

This unit overlies the Woodnamoka formation in the eastern half of the study area as fine- to medium-grained, arkosic sandstone with abundant, heterogeneous clasts. It overlies the Woodnamoka conformably in the east but to the west of the study area the contact is a fault, with strike ridges of Blue Mine Conglomerate bedding into the contact at a moderate to high angle. The clast population is predominantly sub-rounded and composed of quartz, K-feldspar, lithics and volcanic material ranging from coarse sands up to 10 cm in size. Most prominent are small (0.5-3 cm) pale blue quartz clasts visually identical to those seen as porphyroclasts in the Mt. Neill Granite. To the west towards the fault contact quartz augen clasts dominate while the unit also displays thick (>5m) interbeds of felspathic quartzites. Conglomeritic beds in this area display a much higher clast-to-matrix ratio than those in the east with more homogeneous clast populations.

OPAMINDA FORMATION

The dolomites, shales and siltstones of the Opaminda Formation mark the beginning of the more extensive Torrensian deposition in wider rift valleys, with sedimentation onlapping grabens and sediments of older cycles. The unit is typically composed of green actinolitic shales and occasional dolomites, interbedded with dark grey silts which preserve mudcracks and ripple casts. This unit has undergone tight folding with intensity increasing towards the underlying contacts.

Direct contacts between the Opaminda Formation and underlying units are rarely preserved and are primarily picked out by an east-west running creek and its tributaries. The contact between Blue Mine Conglomerate and Opaminda Formation is exposed in one key location to the north of the Sitting Bull Fault. Here the contact is abrupt but conformable with the overlying Opaminda folding sharply into a conformable contact. In similar circumstance, only one outcrop in the west of the study area displays the contact between Wywyana and Opaminda Formations. The lithologies were

identified from each other by grade, with the Wywyana Formation metamorphosed to actinolitic marbles, contrasting with the low grade shales and siltstones of the Opaminda Formation; this location also exhibits a conformable contact. Given the lack of an angular unconformity at this contact but the differential deformation and extent of sedimentation it is most appropriate to describe it as a sedimentary disconformity.

INTRUSIVES

Igneous intrusions of granitic pegmatites and sodic leucogranites outcrop at a number of locations in the study often forming distinct peaks of varying sizes. The most eminent of these are the coarsely crystalline leucogranites of the Pinnacles and Sitting Bull – composed of albite, K-feldspar and quartz. Other intrusions occur in the early Adelaidean sediments, usually through the Wywyana or Paralana, and often near the contact of these units. The most notable of these is the Arkaroola Pegmatite, located to the south of Arkaroola Waterhole. It forms a large, elongate hill (approximately 900 m east-west) and is composed of K-feldspar, quartz and minor phyllosilicates.

3.2 Structural Observations

Like much of the Flinders Ranges, the map pattern of the study area at Arkaroola is dominated by fold interference basins and saddles produced by broad, orthogonal fold phases. The geological mapping of the region has provided structural data and observations with a higher level of detail than previous studies. The Woodnamoka Formation provides an excellent resource for structural data as the schistose rocks record not only the most recent deformational events but also fabrics from earlier tectonic events affecting them, as well as relationships between multiple fabrics. For a

description of sedimentary and tectonic fabrics of the Arkaroola region, as well as the events and structures they are ascribed to see Tables 1 & 2.

3.2.1 DOMINANT SHEAR FABRIC

Care must be taken in structural investigations in multiply deformed terrains to avoid confusing fabrics and lineations of different generations. This applies to the recognition of individual fabrics (and their genesis) as well as identification of corresponding fabrics across multiple locations and lithologies.

The most evident and pervasive fabric in the study area (S_Z) is almost invariably at a low angle (approximately 10-20°) to bedding, maintaining this relationship consistently across the region. This fabric is best observed in pelitic layers of the Woodnamoka Phyllite which have been metamorphosed to amphibolite facies, but lack sufficient aluminium to grow extensive andalusite porphyroblasts. A key location for observation of the early fabrics is an approximately 10-20 m scale synform at the south eastern base of Mt. Oliphant, in Wywyana Creek.

Observations here illustrate that a composite shear fabric has developed before the folding which dominates the map pattern; this fabric is termed S_Z. These pelitic layers commonly show one or two low-angle fabrics of a harmonized orientation. Figure 3 shows the relationships between these fabrics as an early developed fabric (S_{Z1}) is in turn crenulated by a subsequent fabric (S_{Z2}), developed in response to continued shearing in the same orientation. Locally S_{Z2} can be measured as the axial plane to the asymmetric crenulation of S_{Z1}, however in the majority of locations only a single pervasive fabric is recognisable. Composite shape fabrics such as S-C fabrics are infrequently observed. The intersections of foliations with S_0 (bedding) create lineation intersections which, in areas which display an S_{Z2} fabric, are characterised by centimetre scale crenulations on the bedding

surface. It is likely that the observation of a single low angle fabric or multiple fabrics is dependent on the degree, or mode, of strain the rock has experienced.

3.2.2 REGIONAL FOLDING

S_Z is folded with bedding by subsequent deformation, characterised by two orthogonal fold generations termed F_3 and F_4. Bedding measurements taken west of Mt. Oliphant point towards the centre of a large, type 1 fold interference basin forming the dominant large-scale structure of the western map pattern. This is created by a broad F_4 syncline trending approximately NW to SE, coupled with second F_3 fold set with a roughly perpendicular trend; the basin is elongate along the F_4 trend. Stereographic plots of poles to bedding reflect this geometry in varying habits due to location bias of the measurements taken. S_0 readings taken in the Paralana Quartzite and Wywyana Formation reflect their main outcropping patterns on the western and north to north-eastern limbs of the fold interference basin (Figure 4A). The pervasive S_Z fabric shares a similar orientation and low-angle relationship to S_0 and both are shown to be folded by subsequent deformation. Foliations in the basement rocks show a similar orientation to bedding in the overlying sediments (Figure 4B). Projections of S_0 in the Woodnamoka Phyllite exhibit the same fold geometry, with density of readings trending towards the horizontal in the broad, upright centre of the basin (Figure 4C). A fold interference saddle is formed by the NW-SE syncline and F_3 anticline which runs through the peak of Mt. Oliphant and is termed the Mt. Oliphant Anticline. The axial trace of this structure exhibits an arcuate trend with the hinge running roughly east-west before turning approximately SW to NE through the Mt. Oliphant peak.

As discussed, the dominant fabric found in the Adelaidean cover is the S_z shear fabric and no overprinting fabrics occur in orientations that would imply coupling to the broad F_4 folding. However, instances of a dominant fabric forming at a high angle to bedding are intermittently found in course lithologies, particularly the Oliphant Arkose Member. Initially interpreted to correlate with

S_Z, these appear orientated with F_3 fold hinges and it is likely that older fabrics are being overprinted in the coarse units by a pressure solution cleavage that is axial planar to this event. Elburg (2003) has previously noted the occurrence of crenulations in the pelitic beds surrounding Mt. Oliphant but did not ascribe these to an event or fold geometry. Millimetre scale crenulations in the Woodnamoka Phyllite exhibit (Figure 2D) realignment of micas and display a south-westerly fold plunge with an upright axial plane (Figure 5A). Observations of kink banding in layers of the Woodnamoka Phyllite were also made (Figure 2E)

At the type locality for S_Z in Wywyana Creek a 10-20 metre-scale synform provides (outcrop scale) evidence of S_Z fabrics being folded with bedding by subsequent deformation. Millimetre scale crenulations display a crenulation cleavage axial planar to the synform, and lineations of this fabric plunge to the south west. Folding of scales varying from metres to tens of metres are found throughout the Woodnamoka Phyllite in the study area and can be classified as parasitic to F_3.

3.2.3 DELINEATING S_Z WITH RESPECT TO REGIONAL FOLDING

As indicated, the early shear fabrics form differentiated schistosities which have consequently been folded by regional deformation. It is possible to delineate S_Z from the effects of regional folding and examine the orientation of this fabric prior to deformation. Each $L_{Z\text{-}0}$ intersection lineation was rotated by returning the bedding plane (on which it occurred) to the horizontal. A stereographic plot (figure 5B) of these reconstructed lineations shows shallow lines plunging to the north-east and south-west. If this lineation is taken to be a strain sensitive fabric then these trends can provide evidence of the orientation of deformation.

3.2.4 BASEMENT HIGH-STRAIN ZONE

A defining feature of the Proterozoic basement contact with the overlying sediments is a high-strain zone with intense foliation of the granites upwards towards the contact. This granite has previously been described as homogeneous and without fabric, though any fabrics within the Mt. Painter Inlier have been ascribed to Delamerian deformation (Elburg *et al.* 2003). Nevertheless a gradation change in fabric is observed with proximity to the basement unconformity (Figure 6). The fabric ranges from a weak foliation up to approximately 50 m from the contact, through foliated and strongly foliated to a high-strain zone exhibiting grain-size reduction proximal to the contact – this fabric is termed S_ZB (Figure 2B). This pattern is observed throughout the mapping area with the fabric displaying a very low angle (10-15°) to the unconformity (Figure 2F). The granite becomes more muscovite rich as the fabric increases, suggesting retrogression.

The basement foliation displays S-C fabrics and excellent kinematic indicators with quartz phenocrysts (and less frequently K-feldspars) forming sigma-clasts (Figure 2A); ptygmatic quartz veins are also frequently observed. The kinematics consistently display top-to-the-southwest movement to the east of Mt. Oliphant and top-to-the-northeast to the west of Mt. Oliphant.

The low angle geometric relationship between S_Z and bedding in the overlying sediments appears to be mirrored in the relationship between S_ZB and basement-cover unconformity (which is parallel to bedding). The lack of Paralana Quartzite bedding or unconformity measurements at every basement locality means that the basement lineations cannot be reliably unfolded to their original orientation. Despite this, a comparison of stereographic plots (Figure 7) of S_ZB basement lineations and $L_{Z\text{-}0}$ in the overlying sediments shows a strong correlation.

3.2.5 FAULTING

Arkaroola Bore Fault

A fault contact exists in the far east of the study area which has previously been termed the Arkaroola Bore Fault (ABF) (O'Halloran 1992). This structure outcrops in a roughly northeast-southwest line from the Wywyana Formation through to the Woodnamoka Phyllite and places the Wooltana Volcanics unconformably against the Humanity Seat Formation and Arkaroola Creek Breccia Member. The latter lithologies display significant sedimentary thickening toward this structure and neither are present immediately east of the ABF. Both lithologies show thinning away to the west where they pinch out, just south of the Arkaroola Pegmatite.

Sitting Bull Fault

The contact between the Woodnamoka Phyllite and the Blue Mine Conglomerate is conformable in the east of the study area. However this contact is fault bound in the vicinity of Sitting Bull with ridges of Blue Mine conglomerate striking northwest into the fault contact at a high angle; this contact is consequently termed the Sitting Bull Fault (SBF). Here the transitional package between the Woodnamoka and Blue Mine Conglomerate appears to be faulted out by movement along this structure. The fault terminates to the west at the contact with the overlying Opaminda Formation.

Paralana Fault

The Paralana Fault (PF) is part of the Paralana Lineament which has previously (Sandiford *et al.* 1998) been identified as a major crustal structure. Whilst this structure is located outside the eastern extents of the study area it is important to note as it influences some of the observed map patterns. The Woodnamoka Phyllite thickens to the east in a similar manner to Humanity Seat Formation. However, it continues to outcrop extensively to the east of the ECF. Survey mapping (Coats 1973)

adapted by Preiss (1987) shows that the Woodnamoka Phyllite continues to thicken to the east were it abuts the PF.

3.2.6 STRUCTURAL CROSS-SECTIONS

To further investigate the nature of F_3 and F_4 folding, structural cross-sections were produced perpendicular to the major fold axes to ascertain folding geometries (Figure A). The Wooltana 1:50 000 Topographic Series map was used to create topographic profiles whilst bedding readings and foliations have been plotted using apparent dips to the sections.

North Western Transect (section I)

A transect was created perpendicular to the major F_4 syncline to investigate the geometries of the nose of this structure and the folding of the sedimentary package around it. The section through this area (Figure 8) shows that the apparent thickening of both the Wywyana Formation and Paralana Quartzite in the northern limb of the fold can be explained by the sub-horizontal bedding of the sediments in this area. The section also illustrates the nature of the volcanic extrusions showing a low-angle, sill-type geometry cross-cutting the Paralana Quartzite and emplacing within the Wywyana Formation.

North-South and East-West Transects (sections II & V)

Transects were drawn to illustrate the two orthogonal folding events which produced the fold interference basin west of Mt. Oliphant. Sections were produced along, or close to, the hinges of each fold so as to remove it from the section and effectively illustrate the fold set orthogonal to this line. Section II (figure 9) displays the major F_4 syncline as an open, upright, symmetrical fold with sedimentary units remaining at a constant thickness around the hinge. Whilst this section was aligned to be parallel to the F_3 fold hinge through the fold interference basin, the arcuate trend of

the Mt. Oliphant Anticline results in the southernmost part of the section generating a perpendicular view through this fold. This F_3 anticline appears to be have a slightly tighter interlimb angle that the F_4 syncline but overall displays a similar style of open, concentric folding.

Section V was taken sub-perpendicular to the northeast-southwest section II (Figure 10) and shows a broad, upright F_3 syncline forming the fold interference basin. This displays a concentric fold style with a very broad (approximately 130°) interlimb angle. The eastern limb of this fold appears to steepen slightly through the inflection point before folding over into the Mt. Oliphant Anticline. Whilst this fold displays an open, upright fold style in section II, section III shows that it steepened significantly in the hangingwall of the Blue Mine Fault, with the eastern limb of the anticline overturned. This fault has been extrapolated above the surface with the inclination of the fault approximated from the bedding angle of the Woodnamoka above the contact. East of the fault contact the Blue Mine Conglomerate and associated transitional package display continued folding in the F_3 orientation with a return to an open, upright fold style. The overturning of the Mt. Oliphant Anticline and the juxtaposition of the Woodnamoka Phyllite against the Blue Mine Conglomerate may imply that top-to-the-south movement has occurred along this structure.

Central Transect (section III)

A transect was drawn in a rough NNE to SSW orientation, passing approximately 200 m to the east of the Mt. Oliphant peak. The fold interference basin to the west shows no impression on the section (Figure 11) along this line, though the Mt. Oliphant anticline is expressed in the hangingwall of the Sitting Bull Fault. The abutting of the Woodnamoka Phyllite against the Blue Mine Conglomerate along this structure implies this was likely a depositional structure, the Woodnamoka Phyllite forming a localised half-graben. The apparent overturning geometry of the Mt. Oliphant anticline may however imply some later reactivation and ramping along the Sitting Bull Fault.

Eastern Transect (section IV)

A transect was created in a N to S orientation in the eastern part of the study area, from the Ridgetop Track along Wywyana Creek then parallel to the F_3 folding through to the Opaminda Formation. This orientation best illustrates a section through the entire lithology of the region without the influence of any major structures. Figure 12 shows section IV with the entire sequence from the basement contact through the Callanna and Burra sediments dipping to the south at a consistent 45-60° inclination. The angle of the southern portion of the section is such that it removes the effect of the F_3 folding so that no impression of the broad F_4 syncline is observed in the east of the study area.

4. MICROANALYSIS

The differential strain in the Mt Neill Granite, increasing towards the basement-cover unconformity has not been identified by previous workers. Orientated samples were taken from outcrops of the basement high-strain zone for detailed micro-structural analysis. Eleven samples were taken from five sites in the study area with the aim of best representing this rock type across a range of locations, as well as sampling from as close as possible to the contact, where strain levels appears to be highest. Four of these samples were used to produce 30 µm thin sections. The convention used in this analysis is such that the terms sinistral and dextral refer to the kinematics within the orientated sections. The orientation of these sections is known and orientation within them can therefore be applied back to the map pattern.

4.1 Optical Microstructural Analysis

The four thin sections were first used for optical analysis with a Nikon transmitted light microscope. Mineralogical, textural and microstructural observations are described here.

4.1.1 SAMPLE RAK1101

The sample was taken from an area of highly micaceous granite in the far north west of the study area. The outcrop displays a much higher percentage of muscovite than the typical high-strain zone, with the salient feature of the rock being an abundance of large (1-3 cm) K-feldspar porphyroclasts, with large (up to 0.5 cm) muscovites wrapping around them. RAK1101 was sampled from an outcrop of more typical mylonite displaying a measureable lineation, strong grain size reduction and numerous blue quartz porphyroclasts, which had not been destroyed by shearing and showed top-to-the-southwest kinematics.

Optical analysis of the sample showed a mineralogy dominated by quartz, muscovite and biotite as well as the occurrence of large (3-8 mm) K-feldspar porphyroclasts. Worthy of note – though making up less than 2% of the rock – is the occurrence of opaque, euhedral crystals of magnetite, ranging in size from microscopic to approximately 2 mm diameter. The K-feldspar porphyroclasts are predominantly microcline and show strong cross-hatched twinning as well as exhibiting small (0.1-1 mm) inclusions of quartz and muscovites (Figure 13A).

Quartz crystals exist predominantly in lower-strain, but elongate ribbons composed of subgrains commonly display evidence of recrystallisation and grain boundary diffusion (Figure 13B). A second quartz texture is displayed by 3-6 mm blue-quartz porphyroclasts; these exhibit both single quartz grains as well as multiple subgrains, again showing grain boundary diffusion (Figure 13C).

Biotite and muscovite form high-strain domains parallel to the foliation with a strong crenulation displayed by anastomosing low angle fabrics, making it difficult to identify S-C fabrics and shear bands in the section. The fabric also wraps around quartz ribbons and porphyroblasts, in some cases showing asymmetric rotation. In rare instances (Figure 13B) ribbons of quartz can be seen to anastomose around K-feldspar porphyroclasts.

Shear sense defined by rotation of K-feldspar and blue-quartz porphyroclasts is not unequivocally constrained. Many show symmetrical rotation whilst σ-clasts occasionally show a conflicting movement sense as a result of anastomosing nature of the fabric, or localised strain in shear bands. However the vast majority of σ-clasts suggest sinistral movement within the section (Figure 13C).

4.1.2 SAMPLE RAK1103

The sample was taken from the basement unconformity in the north east of the study area on the Ridge Top Track. Outcrops in this area typify the basement high-strain zone, presenting a strong foliation, grain size reduction and regular but relatively sparse porphyroclasts of blue-quartz. Kinematics taken from σ-clasts of these quartz crystals display a top-to-the-southwest movement sense.

Optical analysis of the sample showed a mineralogy completely dominated by quartz, muscovite and biotite, along with very fine (<1 mm) magnetite crystals. Quartz appears predominantly as recrystallised grains in ribbons with widespread grain boundary diffusion (Figure 13D). The sample also features occasional single-grain quartz porphyroclasts of 3-8 mm.

Muscovite and biotite form m-domains of high-strain parallel to the foliation throughout the quartz ribbon texture as well as in long, thin bands (Figure 13D). The fabric anastomoses around quartz ribbons and porphyroclasts, though the sample as a whole shows relatively low strain, lacking wide domains of high strain muscovites and showing symmetrical relationships around porphyroclasts. Given the low strain in the sample, kinematics are inconclusive as to shear sense.

4.1.3 SAMPLE RAK1107

The sample was taken from the type location for the basement unconformity near the Arkaroola Waterhole. Here the Mt Neill Granite is strongly foliated but lacks the significant grain size reduction seen elsewhere. Some large clasts of K-feldspar are still present and the rock, which is described as a proto-mylonite, becomes increasingly micaceous towards the contact.

Optical analysis of the sample shows mineralogy principally composed of quartz, muscovite and biotite, along with very fine (<1 mm) magnetite crystals. Sparse 2-6 mm K-spar clasts are largely overgrown by inclusions of very fine recrystallised quartz and muscovites (Figure 13E). Large porphyroclasts of single grain quartz occur infrequently and the dominant quartz texture is of fine, recrystallised subgrains in low strain packages. These wide (2-10 mm) packages also feature muscovite and biotite and are separated by thin (< 1mm) high strain bands of long muscovite grains forming parallel and sub-parallel to the foliation (Figure 13E). The sample shows a smaller percentage and thinner high strain band of muscovite and biotite than RAK1101 and RAK1103 and as such is lower strain. The section displays rotated quartz porphyroclasts occasionally forming σ-clasts which show a sinistral sense of movement.

4.1.4 SAMPLE RAK1110

The sample was taken from the basement unconformity in the southern side of the Arkaroola Creek, to the northwest of the Arkaroola Waterhole. Here the Mt. Neill Granite forms a mylonite exhibiting strong grain size reduction, development of muscovite and biotite and porphyroblasts of blue-quartz. Kinematics derived from σ-clasts showed a top to the east shear sense.

Optical analysis of the sample revealed mineralogy composed almost entirely of quartz and muscovite, with occasional biotite and rare microscopic grains of magnetite. Quartz is dominantly textured in elongate microlithons of recrystallised grains, frequently showing grain boundary diffusion. These q-domains are punctuated by high strain m-domains parallel to the foliation and composed predominantly of fine grained muscovite (Figure 13F).

An older generation of larger muscovite crystals frequently cross cuts the foliation bands in a harmonized orientation, though these larger crystals also occur parallel to the main fabric. These muscovites appear truncated by the main fabric and belong to an earlier fabric which has been

overprinted (Figure 13G). The section shows considerably higher strain than the previous samples with fluid movement along the shear having all but completely removed K-feldspar and biotite from the original mineralogy of the protolith Mt. Neill Granite. Kinematics displayed by σ-clasts of quartz – both single grain porphyroclasts and those composed of subgrains – exhibit an inconclusive shear sense within the section which appears to be deformed under primarily pure shear (Figure 13H).

4.2 Electron Backscatter Diffraction Analysis

In many cases microstructures within a rock are defined by a preferred orientation of minerals or aggregates within a fabric (Passchier & Trouw 2005). Platelet mineral lineations often form in micas and other planar minerals when a process has aligned these minerals such that they share a common axis. Many rock types exhibit a systematic orientation of crystallographic axes of a mineral, called lattice-preferred orientation (LPO). Through deformation and strain it is possible for equant minerals such as quartz to develop a LPO, however unlike those in micas – which are often recognisable as lineations – this orientation cannot be observed in the field or in optical analysis of thin sections.

One method for the collection of crystallographic preferred orientation (CPO) data is by collecting electron backscatter diffraction patterns (EBSP) from thin sections in a scanning electron microscope (SEM). Two samples were selected from the four Mt. Neill Mylonite thin sections for analysis using EBSD. Samples RAK1103 and RAK1110 were chosen as they represent the lowest and highest observed strain conditions respectively.

4.2.1 METHODOLOGY

The technology to perform microstructural analysis of rock samples using an SEM to map crystallographic orientations has been available for a number of years. In an SEM, an incident beam of electrons creates an omni-directional source of scattered electrons within a specimen. The basis of EBSD is that diffraction of these electrons occurs on the lattice planes of the sample, and the backscattered electrons (those which escape from the sample) form a diffraction pattern which is then imaged on a phosphor screen (Prior *et al.* 1999). Quantitative maps of the crystallographic orientation of individual crystals within a sample can then be constructed from grids of EBSD measurements (Leiss & Weiss 2000). Several papers and reviews (Prior *et al.* 1999, Leiss & Weiss 2000, Lloyd 2000) cover SEM imaging, EBSD, crystallographic orientations, experimental setup and other relevant topics.

4.2.2 ANALYSIS

An outline of the processes of EBSD analysis of thin sections using a SEM and EBSP detector can be found in appendix A.

4.2.3 RESULTS

The results of EBSD CPO mapping for the q-domains of each sample are presented along with the sample's position, orientation in the field and the total number of data points indexed from combined maps for each sample (Table 3). Upper hemisphere equal area projection stereograms and contoured stereograms of c- and a-axes are presented in Figures 15 and 16 and are described below.

Sample RAK1103

An upper hemisphere stereogram projection of quartz c-axes [0001] displays two distinct alignments (Figure 15A). The first are two clusters close to the horizontal and at a low angle to the X-direction of finite strain, illustrating quartz crystals slipping along their c-axis. A second pattern of c-axes distribution shows a dense cluster of data sub-vertical in the Y-direction, with data spreading towards the Z-direction. This pattern is indicative of a mixture of rhomb <a> and prism <a> slip.

Plot [11-20] exhibits the upper hemisphere projection of a-axes; the roughly threefold increase in data points (Figure 15A & B) reflects the crystal structure of quartz having a trigonal spread of 3 a-axes. The pattern observed in Figure 15B shows a distribution of a-axes around the edge of the plot, in sub-horizontal orientations. The dominant clusters are aligned with the lineation in the X-direction, representing the dominant slip along the a-axis in rhomb <a> and prism <a> slip. The sub-horizontal groupings of data towards the Z-direction correspond to the orientation of the other two a-axes, a pattern indicative of prism <a> slip.

Sample RAK1110

The upper hemisphere stereogram plot of quartz c-axes [0001] shows a high density pattern of sub-horizontal alignments with the lineation in the X-direction of finite strain (Figure 16A), though it is possible this density a factor of a abundance of data from a single grain. This pattern of c-axes is indicative of c-slip at a high temperature. A concave girdle of c-axis projections swathes an area from a moderate- to low-angle to the horizontal on the Z-direction to the aforementioned sub-horizontal c-slip cluster. This may denote a progression from primarily rhomb <a> slip shifting to c-slip with an increasing metamorphic grade.

The a-axis plot of this sample Figure 16B shows an essentially inverse pattern to that observed in the projection of c-axes (Figure 16A). This is predicted by the 90° angle between the c-axis and a-axis

plane in the crystal structure of quartz (Figure 14B). The paucity of a-axes plotting in sub-horizontal orientations associated with rhomb <a> slip may add further veracity to the suggestion of a progression from initially rhomb <a> slip to a predominantly c-slip deformational mechanism.

5. DISCUSSION

The tectonic history of the Arkaroola region can be broadly segmented into three main phases: rifting, burial and deformation, and folding. These are discussed below and models for the evolution of the area are proposed.

5.1 Early Cryogenian Rifting and Basin Formation

The considerable thickness of rift, sag and marine sediments within the ARC, coupled with contractional deformation in the Adelaide Fold Belt, means that basins detailing the earliest phases of rifting and sedimentation have been largely buried and obscured (Priess 2000).

The Paralana Lineament has played a critical role in basin formation and deposition of Neoproterozoic rift-phase sediments in the Arkaroola region. Previously identified as a major crustal structure, the Paralana Fault separates the deformed ARC from the Curnamona Craton (Figure 1) (Sandiford *et al.* 1998). Paul *et al.* (1999) asserted that the PF played a significant role in the deposition of Torrensian rift sediments, with depocentres at times located in its hangingwall. McLaren *et al.* (2002) subsequently portray the Paralana Fault as being linked on a regional scale to a fault system penetrating the lithospheric mantle and controlling broad scale deformation, contemporaneous with the Alice Springs Orogeny (ASO). It has been recognised that this structure has a prolonged movement history (Backe *et al.* 2010) and was active during the Mesoproterozoic, as well as during and after Delamerian deformation.. However, overall, the movement history of the Paralana Fault is poorly constrained.

The Paralana Fault bounds the eastern limits of the study area at Arkaroola, with a number of similarly oriented structures exposed to the west. Based on the geometries described in this study, it appears that the ABF, Echo Camp and Northern Fault (NF) may be *en echelon* steps associated with the Paralana Fault system.

Evidence outlined in this paper indicates that the earliest basin development – forming what is here termed the Arkaroola Basin (AB) – was infilled by the Lower Callanna Group comprising the Paralana Quartzite, Wywyana Formation and Wooltana Volcanics. The Willouran landscape in which this basin formed has previously been described as an epicontinental, partially-rifted sag basin (Crawford & Hilyard 1990, Powell *et al.* 1994). The stratigraphy implies a mix of shallow marine, evaporitic and sub aerial depositional (and eruptive) environments. Based on observed structural geometries and the map pattern of the study area, sequential models are proposed for the five stages of rifting and deposition, numbered below in brackets and illustrated in Figure 17.

[1] Two possible models are proposed for the initial opening of a localised rift basin during the Cryogenian.

a) A classic half-graben basin, typical of extensional terranes, with the NF forming the entire western basement-cover contact. This structure would represent a normal fault, with the east-west orientated basement-cover contact in the north of the study area representing the half-graben floor or tilt-block.

b) A pull-apart style basin developed by dilatational jog or a ‘releasing bend’ between stepover strike-slip faults, opened by dextral movement along the Paralana Fault.

[2] A single model is proposed for the next phase of rifting, which resulted in deposition of the Humanity Seat Formation and associated Arkaroola Creek Breccia Member. The extent of these stratigraphic units is bounded by the Echo Camp and ABF. It is proposed that dextral movement along these faults resulted in the textbook-style pull-apart geometry displayed in the map pattern. The thickening relationship of the stratigraphy suggests that the depocentre of this basin was located in the hangingwall of the ABF; the earlier Callanna Group sediments formed the floor of this basin. Whilst the deposition of the Humanity Seat Formation was relatively localised in this region, a greater depositional thickness is localised immediately east of the Paralana Fault. This indicates that the formation of a pull-apart basin to the west of the Paralana Fault was coupled with contemporaneous down-throwing of its eastern block.

[3] The next phase of rifting and deposition is interpreted to have been a result of subsidence along the western side of the Paralana Fault, indicating a reversal of the movement implied by the deposition of the Humanity Seat Formation described above. The distal marine sediments of the Woodnamoka Phyllite thicken easterly into the fault, with the earlier sedimentary sequence forming the basin floor of a half-graben. This was generated by western block down-throwing on the Paralana Fault. The Woodnamoka Phyllite onlaps the earlier rift phases and the gradational contact with the Humanity Seat Formation indicates a lack of a depositional time gap between the two, indicating a paraconformity.

[4] This was followed by a minor phase of rifting characterised by deposition of the Blue Mine Conglomerate in localised half-grabens. The conglomerate in the study area shows thickening relationships toward both the Paralana Fault and Sitting Bull Fault; the latter is interpreted to be a growth fault, which developed during deposition and accounts for the described thickening geometry.

The deposition of the Opaminda Formation represents a widening of the rift zone and a departure from localised deposition in pull-apart basins. The Paralana Fault continued to demarcate the eastern limit of deposition during the broader rift and sag deposition, whilst the Torrens Hinge Zone (Figure 1), a complex, major crustal feature, defined the western limit of the ARC. The outcropping pattern of the Opaminda Formation and Wortupa Quartzite of the upper Emeroo Subgroup demonstrates this broader depositional framework, onlapping the early-rifting AB.

In all, structures observed in the Arkaroola region and the interpretations described above, best fit a model in which *en echelon* stepovers of the Paralana Fault (ABF, ECF and NF) represent fault splays of a strike-slip duplex forming pull-apart extensional basins (Woodcock 1985, Glen 1992, McBride 1994). This geometry is sometimes referred to as a tulip structure and is here termed the Paralana Strike-Slip Duplex (Figure 18).

5.2 Burial & Fabric Development

5.2.1 DEVELOPMENT OF A HIGH STRAIN ZONE AT THE BASEMENT-COVER CONTACT

The previously undescribed high-strain, mylonite-like fabric of the Mt. Neill Granite at the basement-cover contact indicates ductile deformation and in some instances grain size reduction. These fabrics typically form as part of metamorphic core complexes during extension, where detachment faults form a shear zone below the brittle/ductile transition. Continued displacement unroofs the footwall exposing a mylonite zone in the core complex, which is subsequently buried by sediments (Wang & Neubauer 1998). Whilst the geometries of the early basin are not consistent with the development of low-angle detachment faults, a comparable mechanism (at least within a fault plane) is suggested as one possibility for the formation of the observed fabric. Based on field observations and microscopic analysis, shear sense shows top-to-basin movement along the western and north-eastern contacts. Under the second [1b] model of earliest rifting these are interpreted to have

experienced normal movement during basin development. This is consistent with the observed kinematic sense, implying the high-strain zone may have formed synchronously with rifting.

The formation of high-strain fabrics along these structures requires sufficient burial to attain adequate pressure-temperature (PT) conditions to produce ductile deformation. EBSD analysis has shown a strong c-slip mechanism in the deformation of quartz grains, emphasizing the high temperature development of this fabric (Bouchez *et al.* 1986). These conditions typically occur in the mid-crust, with depths of at least 10 km below the earth's surface (Davis & Reynolds 1996). It has previously been established that the high heat producing basement of the Mt. Painter Inlier is associated with elevated middle to upper crustal thermal gradients (McLaren *et al.* 2002). Given the anomalous temperature conditions and an inferred sedimentary thickness of up to 12 km, it is possible to surmise that PT conditions allowing for ductile shearing may have been reached during the final phases of ARC deposition. Therefore it is feasible that syn-sedimentary growth movement along early-rift normal faults produced discrete, high-strain shears. This model accounts for the semi-mylonitic nature of the contact, as well as the opposite kinematic sense observed on either side of the AB.

5.2.2 DEVELOPMENT OF LOW-ANGLE SCHISTOSITIES

The occurrence of a pervasive fabric within the early ARC sediments has been previously documented, and an increase in metamorphic grade to lower amphibolite facies, has been associated with proximity to the Mt. Painter Inlier. This relationship has been described as an "unusual style of unconformity-related contact metamorphism" (Mildren & Sandiford 1995, Sandiford *et al.* 1998). Metamorphism has been recognized as converting pelitic sediments (specifically the Woodnamoka Phyllite) to biotite schists displaying syn- to late-tectonic growth of cordierite and andalusite. The timing and formational mechanism of this earliest and dominant fabric (S_Z) within the early rift sediments is at best, poorly constrained.

Field observations of S_Z illustrate a low-angle geometric relationship to bedding (Figure 3), which remains unchanged across broad scale folding. This is taken to indicate either a complete lack of association with folding of the sedimentary package or an unobserved relationship to a fold event beyond the scale of the study area. Sparse evidence of simple shear indicators coupled with frequent observations of a single low angle fabric are interpreted to suggest a primarily pure shear mechanism, with a progression to non-coaxial deformation.

Relative timing of deformation in the sediments overlying the Mt. Neill Granite has been loosely constrained from observed mineral assemblages and sedimentary thicknesses. McLaren *et al.* (2002) concluded the occurrence of biotite-andalusite-cordierite schists to infer temperature conditions of a least 500°C. Pressure conditions have been estimated at up to 3 kbars, indicated by the widespread andalusite/cordierite-bearing mineral assemblages and inferred crustal depth of 10-12 km (Paul *et al.* 1999). These conditions are correlative with the low pressure, high temperature deformation ascribed to the Delamerian Orogeny (Elburg *et al.* 2003). This deformation associated with the production of S_Z and tectonically correlated andalusite/cordierite-bearing amphibolite facies metamorphism is loosely constrained to post approximately 550 Ma, at which point PT conditions were sufficient to develop the observed mineralogy.

Whilst the exact cause is unclear, it has previously been inferred by Paul *et al.* (1999) that the principal contributor to deformation was the burial of high heat producing basement beneath deep Neoproterozoic basins, producing approximately 40°C km^{-1} geothermal gradients in the upper crust. It is proposed that S_Z formed through the burial of the granitic basement and early rift sequences, leading to temperatures beyond 500°C and pressure conditions of approximately 3 kbars. These conditions were attained by the time rift and sag related deposition had ceased and led to the formation of a planar shear fabric during upper greenschist to amphibolite facies metamorphism.

The exact timing of peak Delamerian-aged deformation in the northern Flinders Ranges is not known. McLaren *et al.* (2002) speculated that peak metamorphism occurred approximately 500 Ma; substantial cooling had occurred by approximately 430 Ma, with hornblende and K-feldspar apparent ages suggesting temperatures of 475°-450°C at this time. The widespread actinolitic alteration observed in the study area occurred above the brittle/ductile transition (Elburg *et al.* 2003) and is localised along faults and stratigraphic contacts. Field observations of entirely actinolitic rocks, deficient of any ductile fabric are ascribed by Elburg *et al.* (2003) to a 440 Ma thermal pulse, providing a broad upper limit on the timing of S_Z and ductile deformation in the region.

Given these broad timing constraints it is difficult to constrain the mechanism and setting of the initial S_Z development accurately. Local variations in coaxial vs. non-coaxial deformation are interpreted to represent progressive deformation (Bell & Rubenach 1983). It is proposed an initial low-angle planar fabric developed under predominately pure shear during peak metamorphism. Progressively non-coaxial deformation is interpreted to have developed during subsequent orogenesis, causing composite shearing which crenulated the earlier fabric (Figure 3). The mechanism for developing a planar fabric at depth is relatively simple. Lithostatic loading through burial generates conditions for ductile deformation with a vertical σ^1 strain axis. Change in the horizontal stress field through extension, contraction, or removal of resistance (essentially a shift from lithostatic equilibrium) can lead to the development of a planar fabric in the lowest strain direction, σ^3. As stated the PT conditions needed to satisfy the mineralogical associations of this fabric would be reached by burial under 10-12 km of sedimentary overburden, thus formation of a planar S_Z likely occurred in response to a change in horizontal or sub-horizontal strain conditions. This may reflect a strain response during pre-Delamerian extension to the onset of orogenesis.

5.2.3 FLUID FLOW IN THE BASEMENT-COVER CONTACT

An alternative model for the development of the high-strain basement fabric may be ascribed to Delamerian-age deformation. The observed increase in muscovite occurrence corresponding to fabric intensity in the basement high-strain zone (Figure 13F) indicates the presence of fluid, most likely sourced from the deformation of the overlying sediments in which pressure solution is interpreted to have played a significant role. This fluid flow at the basement-cover contact likely weakened the basement, creating a feedback between increasing strain and fluid production, leading to the development of a heterogeneously intense high-strain zone. The highest strain sample subjected to optical and EBSD analysis shows almost entirely muscovite dominated m-domains (Figure 13F), highlighting the role of fluid flow in the development of the high-strain zone. EBSD analysis of comparably low and high strain samples indicates the heterogeneous nature of strain intensity and deformational mechanism. The observation of a systematic progression of multiple slip systems in the deformation of quartz grains (Figure 16) can be taken to indicate the progressive nature of deformation in these granites (Passchier & Trouw 2005). The interpretation of a progression from rhomb <a> to c-slip in the high strain sample may be taken as further evidence of progressive deformation, evolving to high temperature, non-coaxial deformation (Peternell *et al.* 2010). This is supported – in contemporaneous development of S_ZB and S_Z – by the occurrence syn-kinematic andalusites, indicating a progression to non-coaxial deformation during peak metamorphism.

5.3 Broad-Scale Structures of the Arkaroola Basin

Regional scale folding of the ARC has been widely documented and investigated (Richert 1976, Drexel *et al.* 1993, Flottmann *et al.* 1994, Marshak & Flottmann 1996, Sandiford *et al.* 1998, Paul *et al.* 1999, Priess 2000, Backe *et al.* 2010). The basement-involved deformation has been primarily attributed to the late Cambrian Del**a**merian Orogeny. The deformation style in the northern Flinders Ranges is dominated by broad, predominantly asymmetric and south verging open folds associated with fault propagation. The majority of shortening appears to be taken up in hangingwall folds and movement along faults (Paul *et al.* 1999).

Field observations of the F_3 and F_4 folding events in the Arkaroola region are consistent with a broad, open style of folding (Figure 9). The overturned nature of the Mt. Oliphant Anticline (Figure 10) was initially interpreted to indicate ramping up along the SBF. The F_4 fold generation is interpreted to reflect the broader folding phase of the northern Flinders Ranges, due to their spatially related hinge trends (Figure 1B). Unfolding this deformation (Figure 19B) illustrates that the overturning geometry is a combination of buttressing of F_3 folds against the Sitting Bull Fault and subsequent re-folding by F_4. The axial trends of F_3 folds are sub-parallel to faults interpreted to define the Paralana Strike-Slip Duplex. This fits a model of fold buttressing against previously depositional structures with fold trends locally reflecting the orientation of faults.

Movement along the Paralana Fault has been inferred as predominantly strike slip (Preiss 1987, Priess 2000, Backe *et al.* 2010), though as a whole it is part of a complex system of faults. A system of stepovers creating synthetic and antithetic splays observed in this study has been interpreted to have formed pull-apart rift basins during dextral strike-slip movement. A reversal of this movement sense to sinistral during the Delamerian (Paul *et al.* 1999) likely inverted these splays, accommodating shortening and deformation controlled by the observed fold sets. This deformation,

whilst reflecting regional stresses, was localised to the AB. Field observations of crenulation cleavages and kink banding (Figure 2D & 2E), spatially associated with F_3, indicates a significant degree of layer parallel shortening during this deformation. This provides further evidence for an anomalous increase in deformation intensity in the AB.

5.4 Models of Tectonic Evolution

A key problem identified from earlier, regional mapping of the Mt. Painter Inlier was the apparent truncation geometry between the south-western limb of what is now identified as a type 1 fold interference basin, and the overlying Opaminda Formation. As described, the lithological contact between the Opaminda Formation and Lower Burra Group is heavily brecciated and rarely outcrops. The variable nature of this contact between broader Torrensian deposition and AB grabens details an apparent change from broad scale folding of greenschist to amphibolite facies metasediments, to the low grade, consistently southward dipping Middle Burra Group in the Arkaroola Region. This relationship is proposed to reflect two possible models of tectonic evolution:

1. A time gap, featuring a probably localised Cryogenian deformational event, before the broader scale deposition of the middle Burra Group.
2. Continuous depositional history between the Willouran and Torrensian sediments with the AB being deformed under localised strain conditions during the regional orogenesis – with the Opaminda Formation acting as a décolement horizon or rheological strain buffer.

The results of this study have provided evidence to support aspects of both of these models. The first model explains the apparent truncation geometry, with a localised deformational event occurring in the mid to late Cryogenian, followed by an erosional time-gap before continued

deposition. The problem with this model is the lack of evidence in the literature for a shortening event during what is broadly interpreted as a phase of widespread rifting. While the F_3 and F_4 fold events appear truncated by the Opaminda Formation, the unequivocal evidence for the development of S_Z preceding these deformations means this model would require a younger than proposed genesis for the shear fabric. The geometry displayed by the broadly deposited Middle Burra Group sediments, onlapping the AB does not conflict with a model of Cryogenian Orogenesis. However, the lack of any obvious unconformable or angular break between the Opaminda Formation and underlying Blue Mine Conglomerate is suggestive of continuous deposition, making it difficult to ascribe this boundary to an orogenic origin.

The second model supports the broadly accepted interpretation of continuous deposition during Cryogenian rifting. It also allows for the formation of S_Z through burial of the early rift sediments before regional deformation, which is seen to broadly fold this fabric in synchronicity with bedding. However this model would then require that the truncation geometry bellow the Opaminda Formation represents a change in, or differing response to, strain conditions. F_3 generation deformation is observed in the map pattern as folding the Opaminda Formation and underlying contact, consistent with a single event having deformed the entire sedimentary sequence. The intense folding observed in the lower Opaminda Formation proximal to the underlying contact, strongly contrasts with the comparatively unfolded sediments at the top of the formation. The arcuate fold traces of F_3 curve west into the Opaminda Formation, before tapering out. This is taken to indicate the Opaminda Formation may have acted as a rheological buffer, or décollement horizon, taking up strain through shear movement (Figure 19B) and accounting for the disparity in local and regional deformation intensity. This model of tectonic evolution effectively explains the apparent truncation of broad-scale folding observed between the AB and the overlying Middle Burra Group sediments.

5.4.1 GEOMETRIES OF CONSTRICTIONAL DEFORMATION

Mineral lineations form in deformed rocks as a response to differential stress. In the Mt. Neill Granite, elongate muscovite and biotite grains define a lineation of this nature, which commonly, but not always, form parallel to the maximum strain direction. Figure 7 illustrates that mineral lineations in the basement and intersection lineations in the cover (predominately the Woodnamoka Phyllite) show a strongly correlative NE to SW orientation; this orientation is reflected by the trend of the F_3 fold generation. In a typical compressional regime, mineral lineations will form sub-perpendicular to fold trends and crenulations, in the direction of tectonic transport. However, rocks documenting the mid-crust levels of orogenic terranes frequently display a relationship of parallel, or sub-parallel fold hinges and stretching lineations (Ridely 1986).

Bends and stepovers in strike slip faults tend to form regions of anomalous deformation (McBride 1994). These strike-slip terranes, like the Paralana Fault system broadly have a vertical σ^2 direction, which can lead to constrictional deformation (Ferrati *et al.* 1996, Wang & Neubauer 1998, Poli & Oliver 2001, Williams & Jiang 2005). This is interpreted to have occurred as F_3 folds, buttressed against faults (Figure 19), elongate in the direction of minimum strain, parallel to fold hinges. This hinge parallel σ^3 direction essentially becomes the direction of extension, forming mineral stretching lineations parallel to fold trends in appropriate lithologies. It is therefore possible that the observed lineations and F_3 fold trends correspond to the same progressive deformation.

6. CONCLUSIONS

The AB displays a structural record incongruous with the broad scale history of the northern Flinders Ranges. Following a detailed structural investigation, it appears that the primary factor controlling deposition and deformation in the Arkaroola region was the formation of a strike-slip duplex. This duplex formed during the earliest rifting related to the break-up of Rodinia, elsewhere interpreted to be *ca* 830 Ma. The Paralana Fault was active during this period with dextral movement forming a duplex of synthetic and antithetic fault splays, leading to the polyphase opening of localised pull-aparts, comprising the AB.

Anomalously high heat producing basement rocks coupled with burial of the Callanna and Lower Burra Groups by subsequent rift and sag phase deposition is interpreted to have produced PT conditions in excess of 500-550° C and approximately 3 kbars. These were sufficient to accommodate for amphibolite grade metamorphism, coupled with the formation of planar burial fabric pre-dating regional folding. Rotated syn-kinematic andalusites and progressive shear crenulations indicate this fabric likely evolved with an increasingly simple shear component during the Delamerian Orogeny. A previously undefined high-strain zone at the basement-cover contact is interpreted to have formed through fluid flow during progressive deformation. Observations in this study combined with data from previous workers place broad constraints on the development of S_Z to between the cessation of rifting and a 440 Ma thermal pulse.

The sedimentary sequence and S_Z fabric were subsequently folded by F_3 and F_4 fold phases. F_3 displays arcuate fold axes which are spatially restricted to the AB sediments. This deformation is not evident above the Opaminda Formation which has accommodated strain through shear movement, parallel to bedding. This model accommodates the disparity in shortening observed (underscored by layer parallel shortening) in the AB comparative to the overlying sediments.

The alignment of mineral lineations and deformational structures with the F_3 fold trend is attributed to constrictional deformation creating extension along fold hinges parallel to faults. The F_3 folds are buttressed against previously depositional structures of the Paralana Strike-Slip Duplex, reactivated by sinistral movement on the Paralana Fault during the Delamerian Orogeny, localising deformation of the AB. The apparent truncation of folding in conjunction with differential shortening can be explained by localisation within duplex-bounding faults.

7. ACKNOWLEDGEMENTS

This study could not have been undertaken without the support and hospitality of Doug and Marg Sprigg, as well as the friendly staff of the Arkaroola Resort and Wilderness Sanctuary. Thanks must go to my supervisors David Giles and Alan Collins for their invaluable assistance in the field and many enlightening discussions on geological problemati*ca* Thanks go to Ben Wade for his expert assistance the use of the SEM and EBSP detector and (the imminently Dr.) Katie Howard for read-throughs and any number of pointers of producing a legible thesis. Special thanks go to Ashleigh Job for making the weeks of remote field work tolerable. Thanks to my family and friends who have supported me through the year and finally to mum for many proof-reads, suggestions and raised eyebrows.

8. REFERENCES

BACKE G., BAINES G., GILES G., PREISS W. & ALESCI A. 2010. Basin geometry and salt diapirs in the Flinders Ranges, South Australia: Insights gained from geologically-constrained modelling of potential field data. *Marine and Petroleum Geology* **27**, 650-665.

BELL T. H. & RUBENACH M. J. 1983. Sequential Porphyroblast Growth and Crenulation Ceavage Development During Progressive Deformation *tectonophysics* **92**, 171-194.

BOUCHEZ J. L., MAINPRICE D., BLUMENFELD P. & TUBIA J. M. 1986. Dominant *c* slip in naturally deformed quartz: Implications for dramatic plastic softening at high temperature. *Geology* **14**, 819-822.

BURKE K. & DEWEY J. F. 1973. Plume-Generated Triple Junctions:Key Indicators in Applying Plate Tectonics to Old Rocks. *Journal of Geology* **81**, 406-433.

CAWOOD P. A. 2005. Terra Australis Orogen: Rodinia breakup and development of the Pacific and Iapetus margins of Gondwana during the Neoproterozoic and Paleozoic. *Earth-Science Reviews* **69**, 249-279.

COATS R. P. 1973. COPLE, South Australia, sheet SH54-9. *South Australian Geological Survey, 1:250 000 series, Explanitory Notes*.

CRAWFORD A. J. & HILYARD D. 1990. Geochemistry of Late Proterozoic flood basalts, Adelaide Geosyncline, South Australia. *Geological Society of Australia* **Special Publication No. 16**, 49-67.

DAVIS G. H. & REYNOLDS S. J. 1996. *Structural Geology of Rocks and Regions*. John Wiley & Sons, Inc. .

DREXEL J. F., PREISS W. V. & PARKER A. J. 1993. The Geology of South Australia. *Precam. S. Aust. Geol. Surv. Bull. 54* **1**.

ELBURG M. A., BONS P. D., FODEN J. & BRUGGER J. 2003. A newly defined Late Ordovician magmatic–thermal event in the Mt Painter Province, northern Flinders Ranges, South Australia. *Australian Journal of Earth Sciences* **50**, 611.

FERRATI L., OLDOW J. S. & SACCHI M. 1996. Pre-Quaternary orogen-parallel extension in the Southern Apennine belt, Italy. *tectonophysics* **260**, 325-347.

FLOTTMANN T., JAMES P., ROGERS J. & JOHNSON T. 1994. Early Palaeozoic foreland thrusting and basin reactivation at the Palaeo-Pacific margin of the sutheastern Australian Precambrian Craton: a reappraisal of the structural evolution of the Southern Adelaide Fold-Thrust Belt. *tectonophysics* **234**, 95-116.

FODEN J., ELBURG, M.A., DOUGHERTY-PAGE J. & BURTT A. 2006. The Timing and Duration of the Delamerian Orogeny: Correlation with the Ross Orogen and Implications for Gondwana Assembly. *Journal of Geology* **114**, 189-210.

FORBES B. G., MURRELL B. & PREISS W. 1981. Subdivision of the lower Adelaidean, Willouran Ranges. *South Australian Geol. Survey Quart. Geol.* **Notes 79**, 7-16.

GLEN R. A. 1992. Thrust, extensional and strike-slip tectonics in an evolving Palaeozoic orogen - a structural synthesis of the Lachlan Orogen of southeastern Australia. *tectonophysics* **214**, 341-380.

HILYARD D. 1990. Willouran Basin Province: Straitgraphy of Late Proterozoic flood basalts, Adelaide Geosyncline, South Auastralia *Geological Society of Australia* **Special Publication No. 16**, 34-48.

HOFFMAN P. F. 1991. Did the breakout of Laurentia turn Gondwanaland inside-out? . *Science* **252**, 1409-1412.

HOUSEMAN G. A. 1990. The thermal structure of mantle plumes: axisymmetric or triple-junction? *Geophys. J. Int.* **102**, 15-24.

HOUSEMAN G. A. 1991. The Triple-junction Structure of Mantle Plumes and Contiental Rifting`. *Exploration Geophysics* **22**, 195-198.

LEISS B. & WEISS T. 2000. Fabric anisotropy and its influence on physical weathering of different types of Carrara marbles. *Journal of Structural Geology* **22**, 1737-1745.

LI Z. X., BOGDANOVA S. V., COLLINS A. S. D., A., WAELE B. D., ERNST R. E., FITZSIMONS I. C. W., FUCK R. A., GLADKOCHUB D. P., JACOBS J., KARLSTROM K. E., LU S., NATAPOV L. M., PEASE V., PISAREVSKY S. A., THRANE K. & VERNIKOVSKY V. 2008. Assembly, configuration, and break-up history of Rodinia: A synthesis *Precambrian Research* **160**, 170-210.

LI Z. X., LI X. H., KINNY P. D. & WANG J. 1999. The breakup of Rodinia: did it start with a mantle plume beneath South China? *Earth and Planetary Science Letters* **173**, 171-181.

LI Z. X., ZHANG L. & POWELL C. M. 1995. South China in Rodinia: Part of the missing link between Australia-East Anatartica and Laurentia? *Geology* **23**, 407-410.

LINDSAY J. F., KORSCH R. J. & WILFORD J., R. 1987. Timing the breakup of a Proterozoic supercontinent: Evidence from Australian intracrationic basins. *Geology* **15**, 1061-1064.

LLOYD G. E. 2000. Grain boundary contact effects during faulting of quartzite: an SEM/EBSD analysis. *Journal of Structural Geology* **22**, 1675-1693.

MARSHAK S. & FLOTTMANN T. 1996. Structure and origin of the Fleurieu and Nackara Arcs in the Adelaide fold-thrust belt, South Australia: salient and recess development in the Delamerian Orogen. *Journal of Structural Geology* **18**, 891-908.

MAWSON D. & SPRIGG R. C. 1950. *Austral. J. Sci.* **13**, 69.

MCBRIDE J. H. 1994. Investigating the crustal structure of a strike-slip "step-over" zone along the Great Glen fault. *Tectonics* **13**, 1150-1160.

MCLAREN S., DUNLAP J. W., SANDIFORD M. & MCDOUGALL I. 2002. Thermochronology of high heat-producing crust at Mount Painter, South Australia: Implicatios for tectonic reactivation of continental interiors. *Tectonics* **21**.

MILDREN S. D. & SANDIFORD M. 1995. Heat refraction and low-pressure metamorphism in the northern Flinders Ranges. *Australian Journal of Earth Sciences* **42**, 241-247.

O'HALLORAN G. 1992. The evolution of provenance and depositional processes during earlier Adelaidean sedimentation: sedimentalogical and Nd isotopic investigation. Bachelor of Sciences (Hons) thesis, Geology & Geophysics, The University of Adelaide, Adelaide (unpubl.).

PASSCHIER C. W. & TROUW R. A. J. 2005. *Microtectonics* Springer.

PAUL E., FLOTTMANN T. & SANDIFORD M. 1999. Structural geometry and controls on basement-involoved deformation in the northern Flinders Ranges, Adelaide Fold Belt, South Australia. *Australian Journal of Earth Sciences* **46**, 343-354.

PETERNELL M., HASALOVA P., WILSON C. J. L., PIAZOLO S. & SCHULMANN K. 2010. Evaluating quartz crystallogaphic preffered orientations and the role of deformational partitioning using EBSD and fabric analyser techniques *Journal of Structural Geology* **32**, 803-817.

PISAREVSKY S. A., WINGATE M. T. D., POWELL C. M., JOHNSON S. & EVANS D. A. D. 2003. Models of Rodinia assembly and fragmentation. *Geological Society, London, Special Publications* **206**, 35-55.

POLI L. C. & OLIVER G. J. H. 2001. Contrictional deformation in the Cental Zone of the Damara Orogen, Nambia. *Journal of African Earth Sciences* **33**, 303-321.

POWELL C. M., PRIESS W. V., GATEHOUSE C. G., KRAPEZ B. & LI Z. X. 1994. South Australian record of a Rodinian epicontinental basin and its mid-Neproterozoic breakup (~700 Ma) to form the Palaeo-Pacific Ocean

tectonophysics **237**, 113-140.
PREISS W. V. 1982. Supergroup classification in the Adelaide Geosyncline. *Trans. Roy. Soc. South Australia* **106**, 81-83.
PREISS W. V. 1987. The Adelaide geosyncline: Late Proterozoic stratigraphy, sedimentation, palaeontology and tectonics. *Bull. Geol. Surv. South Aust.* **53**.
PREISS W. V., DYSON I. A., REID P. W. & COWLEY W. M. 1998. Revision of lithostraticgraphic classification of the Umberatana Group. *MESA* **9**, 36-42.
PRIESS W. V. 2000. The Adelaide Geosyncline of South Australia and its significance in Neoproterozoic continental reconstruction. *Precambrian Research* **100**, 21-63.
PRIOR D. J., BOLYE A. P., BREKNER F., CHEADLE M., DAY A., LOPEZ G., PERUZZO L., POTTS G. J., REDDY S., SPIESS R., TIMMS N. E., TRIMBY P., WHEELER J. & ZETTERSTROM L. 1999. the application of electron backscatter diffration and orientation contrast imaging in the SEM to textural problems in rocks. *American Mineralogist* **84**, 1741-1759.
RICHERT J. P. 1976. Thrust faulting in the northern flinders range, South Australia. *Journal of the Geological Society of Australia* **23**, 361-366.
RIDELY J. 1986. Parallel stretching lineations and fold axes oblique to a shear displacment direction - a model and observations. *Journal of Structural Geology* **8**, 647-653.
SANDIFORD M., PAUL E. & FLOTTMANN T. 1998. Sedimentary thickess variations and deformation intensity during basin enversion in the Flinders Ranges, South Australia. *Journal of Structural Geology* **20**, 1721-1731.
THOMPSON B. P., COATS R. P., MIRAMS R. C., FORBES B. G., DALGARNO C. R. & JOHNSON J. E. 1964. Precambrian rock groups in the Adelaide Geosyncline: a new subdivision. *Geological Notes, Geol. Surv. S. Austr.* **9**, 1-19.
WANG J. & LI Z. X. 2003. History of Neoproterozoic rift basins in South China: implications for Rodinia break-up. *Precambrian Research* **122**, 141-158.
WANG X. & NEUBAUER F. 1998. Orogen-parallel strike-slip faults bordering metamorphic core complexes: the Salzach-Enns fault zone in the Eastern Alps, Austria. *Journal of Structural Geology* **20**, 779-818.
WANG X. C., LI X. H., LI Z. X., LIU Y. & YANG Y. H. 2010. The Willouran basic province of South Australia: Its relation to the Guibei large igneous province in South China and the breakup of Rodinia. *Lithos* **119**, 569-584.
WILLIAMS P. F. & JIANG D. 2005. An investigation of lower crustal deformation: Evidence for channel flow and its implications for tectonics and structural studies. *Journal of Structural Geology* **27**, 1486-1504.
WINGATE M. T. D., CAMPBELL I. H., COMPSTON W. & GINBSON G. M. 1998. Ion microprobe U-Pb ages for Neoproterozoic basaltic magmatism in south-central Australia and implications for the breakup of Rodinia. *Precambrian Research* **87**, 135-159.
WOLFENDEN E., EBINGER C., YIRGU G., DENINO A. & AYALEW D. 2004. Evolution of the northern Main Ethiopian rift: birth of a triple junction. *Earth and Planetary Science Letters* **224**, 213-228.
WOODCOCK N. H. 1985. Strike-slip duplexes. *Journal of Structural Geology* **8**, 725-735.

9. LIST OF TABLES

10. FIGURE CAPTIONS

Figure A. Geological map of the Arkaroola Basin in the northern Flinders Ranges. Map was completed at 1:10 000 scale using geo-rectified Quickbird satellite imagery as a base for field mapping and digitised using CorelDRAW X4 software. (a) Tectonic sketch of the Arkaroola Basin showing major fault movement during extension and basin formation.

Figure 1. (a) Geological map of the South Australian Adelaide Rift Complex and its major constituents. The Torrens Hinge Zone demarcates the western limit of the ARC with the Gawler Craton whilst the Paralana Fault bounds the northern Flinders Ranges from the Curnamona Craton in the east. (b) Regional geological map of the Mt. Painter Inlier and Neoproterozoic sedimentary sequence of the northern Flinders Ranges, study area at Arkaroola marked by box; adapted from Elburg (2003), Paul (1999) and Drexel *et al.* (1993). PF, Paralana Fault; NWF, Norwest Fault; US, Umberatana Syncline; YA, Yankannina Anticline; AS, Arkaroola Syncline; GDS, Gairdner Dyke Swarm.

Figure 2. (a) Quartz augen in high-strain zone of Mt. Neill Granite near the basement-cover contact; (b) erosional unconformity between basement Mt. Neill Granite and overlying Paralana Quartzite; (c) Arkaroola Creek Breccia Member of the Humanity Seat Formation showing heterogeneous clast

population; (d) fine-scale crenulations of S_Z fabric in the Woodnamoka Phyllite; (e) kink banding in Woodnamoka Phyllite; (f) low angle fabric of high-strain zone proximal to the basement-cover contact.

Figure 3. (a) Annotated photograph of angular relationships of composite fabric (S_{Z1} & S_{Z2}) in the Woodnamoka Phyllite; (b) sketch of photograph displaying relationship of composite fabric to lineation and bedding.

Figure 4. Lower-hemisphere stereogram projection of (a) densities of poles to bedding of Paralana Quartzite and Wywyana Formation bedding reflecting western and north-north-eastern limbs of the fold interference basin; (b) density of poles to foliation planes in the Mt. Neill Basement, these are taken to be spatially equivalent to S_Z and show a similar reflection of fold limbs; (c) densities of poles to bedding in Woodnamoka Phyllite displaying a trend towards the sub-horizontal bedding of the centre of the fold interference basin.

Figure 5. Lower-hemisphere stereogram projection of (a) poles to S_3 fabric, axial to millimetre scale crenulations, indicating upright folding with a roughly southwest-northeast trend (squares) and lines of millimetre scale crenulations ($L_{3\text{-}Z}$) displaying south-westerly plunge of F_3 folding (triangles); (b) densities of S_Z lineations rotated to original orientation by rotating S_0 to the horizontal.

Figure 6. (a) Annotated photograph of basement-cover contact above Arkaroola Creek displaying (1) thick basal Paralana Quartzite, (2) high-strain zone and (3) foliated granite; (b) sketch of photograph illustrating decreasing fabric intensity away from the basement-cover contact.

Figure 7. Lower-hemisphere stereogram projection of (a) densities of lines of mineral lineations in the basement high-strain zone, with a higher density of points in the south-west due to sampling

location bias; (b) densities of lines of intersection lineations ($L_{Z\text{-}0}$) in the Woodnamoka Phyllite. Overlapping orientations illustrate a spatial equivalency between S_Z and S_ZB.

Figure 8. Vertical cross-section along transect line I-I' displaying broad F_4 syncline of fold the interference basin, sub-horizontal bedding to the north and sill-type extrusion of Wooltana Volcanics through the Paralana Quartzite and into the Wywyana Formation.

Figure 9. Vertical cross-section along transect line II-II' displaying broad, upright F_4 syncline of fold interference basin and broad, upright Mt. Oliphant Anticline along the east-west trending section of its arcuate hinge.

Figure 10. Vertical cross-section along transect line V-V' displaying F_4 syncline, overturned Mt. Oliphant Anticline to the north of the Sitting Bull fault, which (projected above surface) constitutes an angular unconformity between the Woodnamoka Formation and the Blue Mine Conglomerate. These units are separated by a transitional package where the contact between them is conformable.

Figure 11. Vertical cross-section along transect line III-III' displaying overturned Mt. Oliphant Anticline north of the Sitting Bull Fault (projected above surface). Broad F_4 syncline shows no impression on this section as the entire sedimentary sequence shows a consistently southward dipping orientation of bedding.

Figure 12. Vertical cross-section along transect line IV-IV' displaying entire sedimentary sequence from the basement-cover contact to the Opaminda Formation with the effects of folding removed by the transect orientation.

Figure 13. (a) Alkali-Feldspar (microcline) porphyroclast in thin section RAK1101 displaying overgrowth by quartz and muscovite; (b) q-domains of recrystallised quartz subgrains showing grain boundary diffusion, while q-domains wrap around K-feldspar porphyroclasts; (c) grain boundary diffusion in a quartz porphyroclast forming a σ-clast illustrating a sinistral movement sense within the section; (d) partitioning of strain in sample RAK1103 between quartz subgrains in q-domains and muscovite and biotite in m-domains; (e) porphyroclast of K-feldspar (bottom) overgrown by quartz and muscovite while foliation-parallel m-domains anastomose around q-domains; (f) distinct strain partitioning into m-domains composed almost entirely of muscovite in sample RAK1110; (g) large muscovite grain of an early fabric cross-cut and truncated by foliation-parallel m-domains; (h) quartz porphyroclast in sample RAK1110 showing inconclusive movement sense, likely due to a predominantly pure shear deformational mechanism.

Figure 14. (a) Schematic orientation of a quartz crystal in the reference field constrained by a foliation (S_r) and a lineation (L_r) with the angles α and β defining the orientation of the quartz c-axis from these reference planes; (b) schematic of upper-hemisphere stereogram projection of the quartz c-axis in (a), plot point defined by the angles α and β; (c) crystal structure of a quartz crystal illustrating angular relationship between c-axis and trigonal a-axes; adapted from Passchier & Trouw (2005).

Figure 15. Sample RAK1103 upper-hemisphere, equal area stereogram plots of (a) quartz c-axes displaying two distinct patterns, one of c-slip and the other of combination rhomb <a> and prism <a> slip deformational mechanisms; (b) quartz a-axes displaying patterns indicative of prism <a> slip deformational mechanisms. Each plot is reproduce below the original with a density contour.

Figure 16. Sample RAK1110 upper-hemisphere, equal area stereogram plots of (a) quartz c-axes displaying a dominant c-slip deformational mechanism as well as a partial girdle across the top of the

plot indicating a possible progression between rhomb <a> slip and c-slip; (b) quartz a-axes displaying a lack of sub-horizontal data associated with rhomb <a> slip and a sub vertical density indicating a predominantly c-slip deformational mechanism. Each plot is reproduce below the original with a density contour.

Figure 17. Schematic cartoons detailing proposed models for major depositional phases of the rifting history of the Arkaroola basin: [1a] earliest rifting and Callanna group deposition in a classic half-graben style basin controlled by normal faulting along what is now the western margin of the basin; [1b] alternative rift initiation of a pull-apart style basin formed by dextral movement along the Paralana Fault and associated stepovers creating a dilational jog; [2] deposition of the Humanity Seat Formation accommodated by dextral movement along the ABF and ECF forming a localised pull-apart basin, floored by the earlier Callanna Group; [3] deposition of the Woodnamoka Phyllite accommodated by down-throwing of the western side of the Paralana Fault, onlapping the earlier sequences; [4] localised deposition of the Blue Mine Conglomerate accommodated by continued subsidence on the western side of the Paralana Fault and growth movement on the Sitting Bull Fault representing a different orientation of faulting. Depositional environments are indicated as [1] shallow marine, lacustrine, evaporitic and aerial to sub-aerial volcanism; [2] shallow marine; [3] shallow to distal marine and lacustrine; [4] proximal shallow marine and marine rock fall.

Figure 18. Schematic comparison between (a) a textbook example of pull-apart basin formation in a strike slip fault system adapted from Davis & Reynolds (1996); (b) three dimensional tectonic sketch of Arkaroola Basin with inferred strike-slip duplex geometry formed during dextral movement along the Paralana Fault and associated *en echelon* stepovers.

Figure 19. Schematic cross-section of (a) modern day orientation of rocks along a north-west trending idealised transect through the Sitting Bull Fault and overturned Mt. Oliphant Anticline, with

topography in red; (b) restored section with the effects of F_4 folding removed displaying the buttressing geometry of F_3 folds, intensity increasing towards the steeply dipping, normal Sitting Bull Fault. F_3 fold trends arc into overlying Opaminda Formation before tapering out suggesting the Opaminda Formation accommodated strain via a shear mechanism.

11. TABLES

Table 1.

FABRIC	DESCRIPTION OF FABRIC AND FORMATION MECHANISM
S_0	Bedding of sedimentary sequence
S_Z	Composite fabric pre-dating folding
S_ZB	Foliation in high-strain zone at basement-cove contact
L_ZB	Mineral stretching lineation defined by micas in S_ZB plane
S_{Z1}	Initial planar component of S_Z
S_{Z2}	Progressive deformation of S_Z, crenulates S_{Z1}
L_{Z-0}	Intersection lineation of S_Z on S_0
S_3	Axial plane of millimetre crenulations associated with F_3 folding
L_{3-Z}	Intersection of millimetre crenulations on S_Z

Table 2.

TECTONIC EVENT	ASSOCIATED FABRIC	ASSOCIATED STRUCTURES
Rifting & Deposition	S_0	Sedimentary structures, faults bounding rift basins
Burial & pure shear	S_{Z1}	-
Progressive deformation	S_{Z2}, L_{Z-0}, S_ZB, L_ZB	Crenulations of S_Z, high-strain zone at basement-cover contact
Progressive deformation, fault reactivation and localised folding	S_3, L_{3-Z}	F_3 folding
Regional folding	-	F_4 folding

Table 3.

Sample No.	Sample Location (GPS)	Foliation (dip/dip dir.)	Lineation	No. Data Points Indexed	Active Slip Systems
RAK1103	0340987 E 6649238 N	84/140	52→255	162536	Rhomb <a> slip, Prism <a> slip, c-slip
RAK1110	0339527 E 6648979 N	47/231	41→235	198010	Rhomb <a> slip, c-slip

Figure 1.

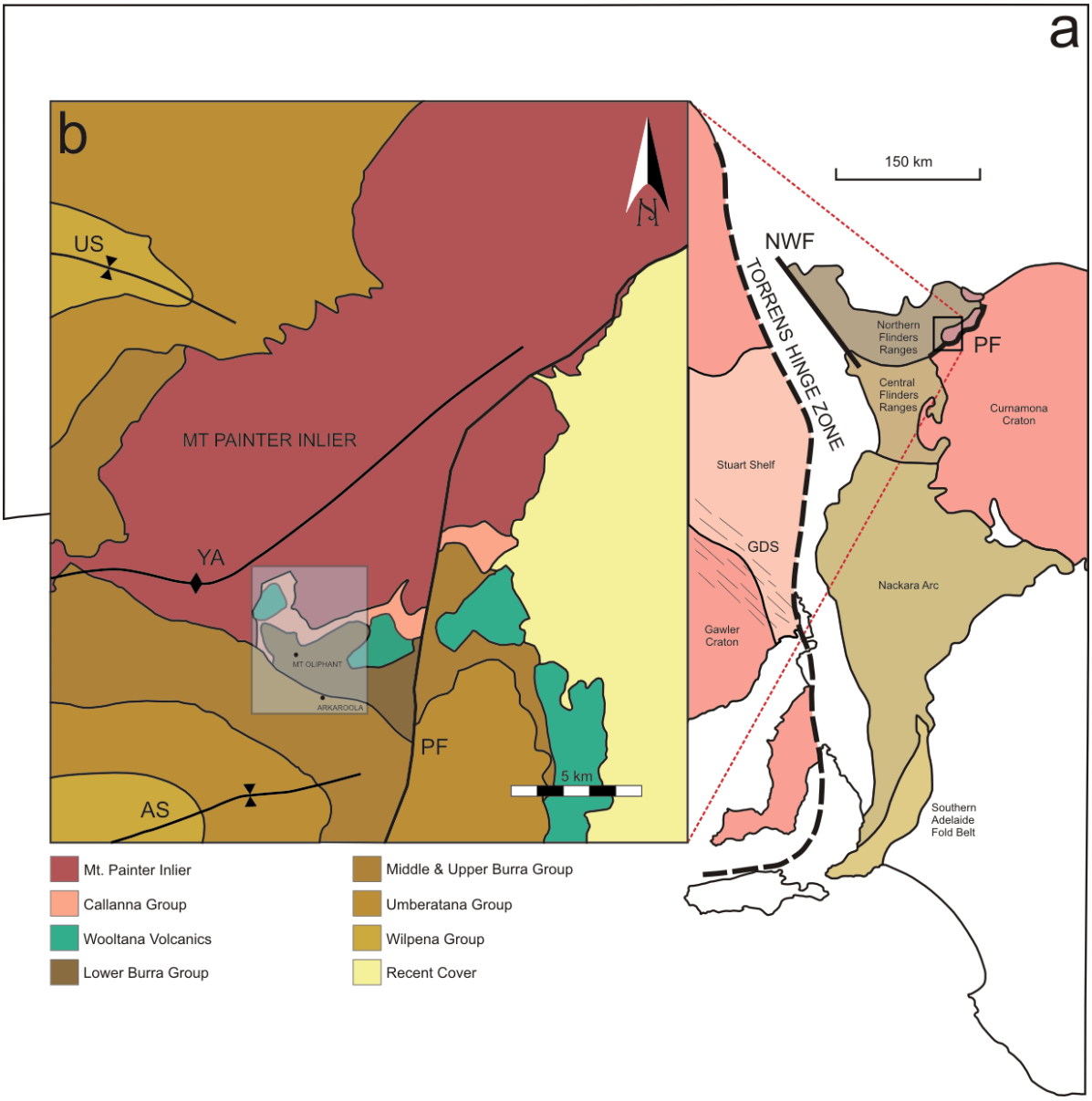
a
b
150 km
N
US
NWF
TORRENS HINGE ZONE
Northern Flinders Ranges
PF
Central Flinders Ranges
Curnamona Craton
MT PAINTER INLIER
Stuart Shelf
YA
GDS
Nackara Arc
Gawler Craton
MT OLIPHANT
ARKAROOLA
PF
5 km
AS
Southern Adelaide Fold Belt
Mt. Painter Inlier
Callanna Group
Wooltana Volcanics
Lower Burra Group
Middle & Upper Burra Group
Umberatana Group
Wilpena Group
Recent Cover

Figure 2.

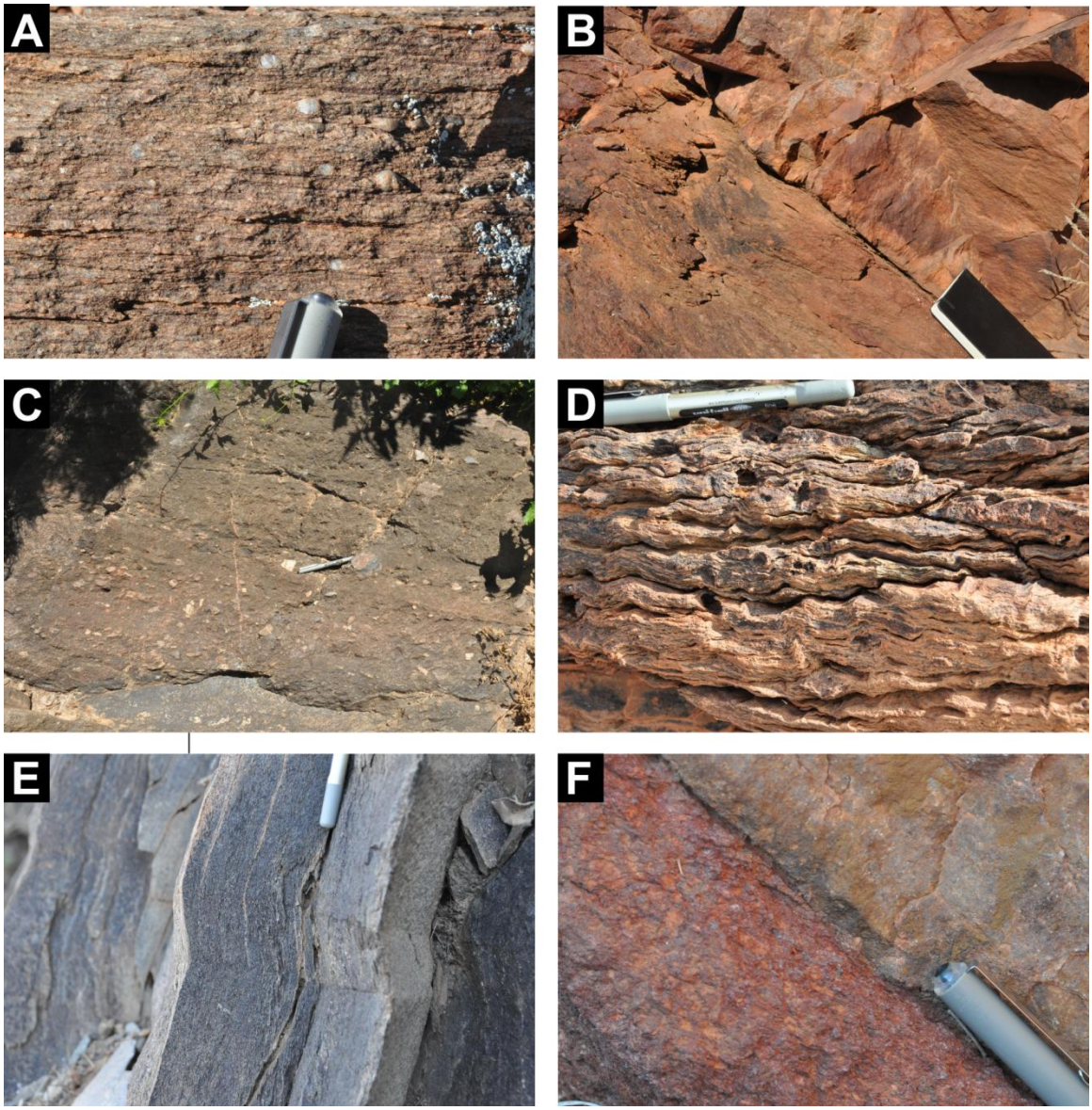

Figure 3.

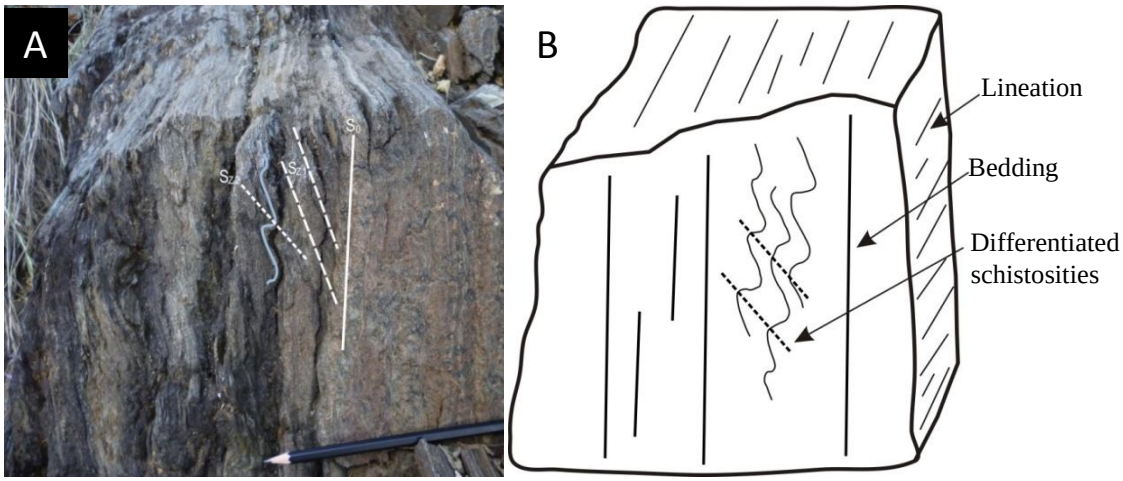

Figure 4.

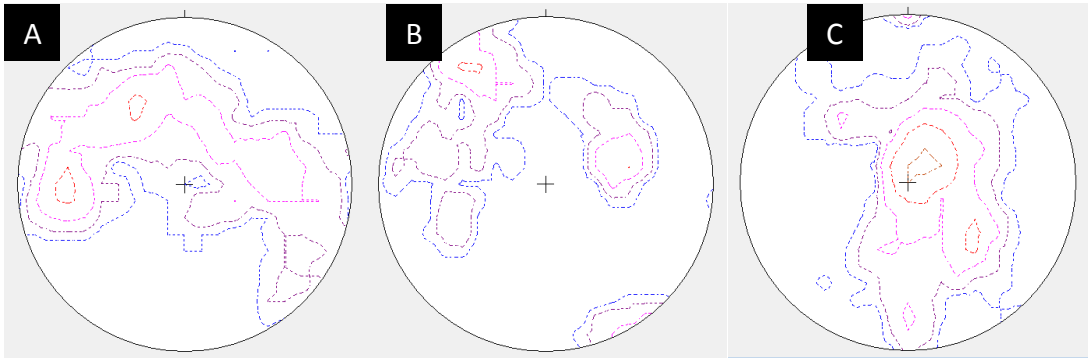

Figure 5.

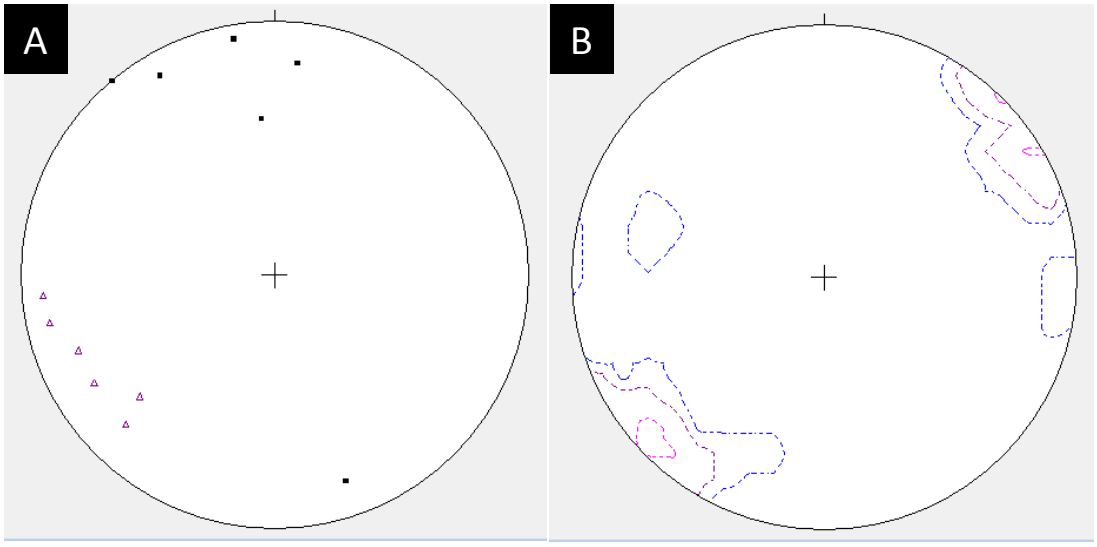

Figure 6.

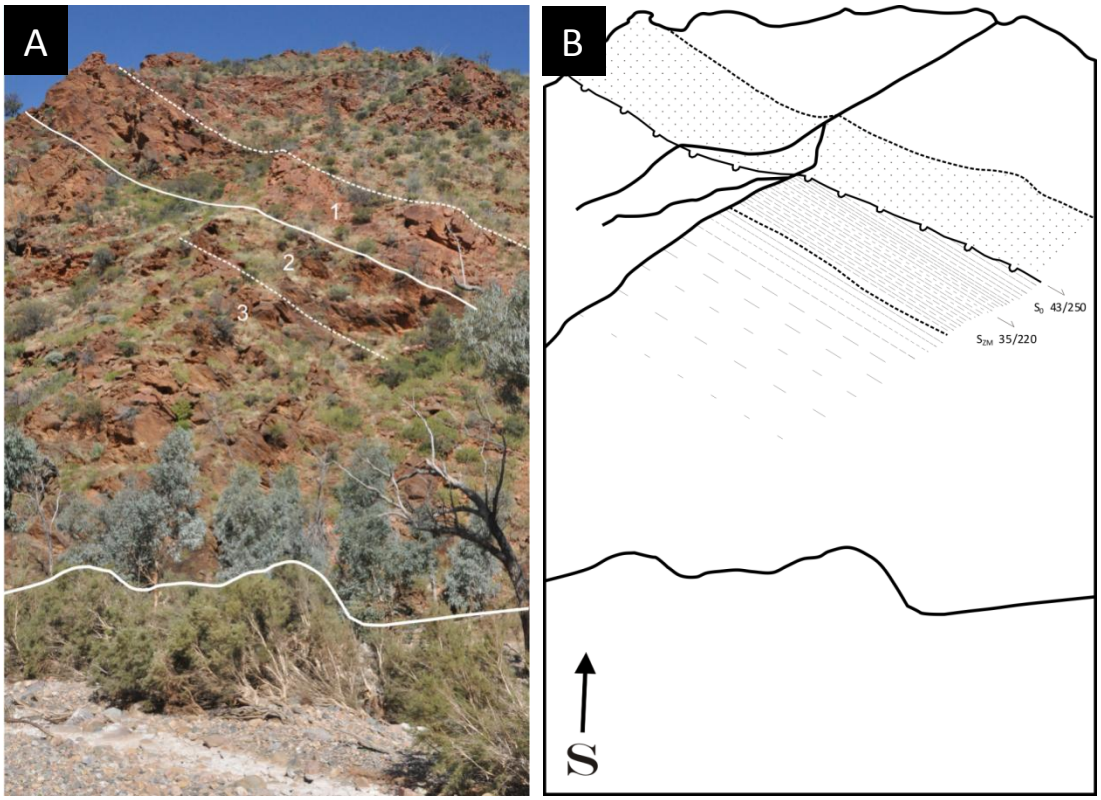

Figure 7.

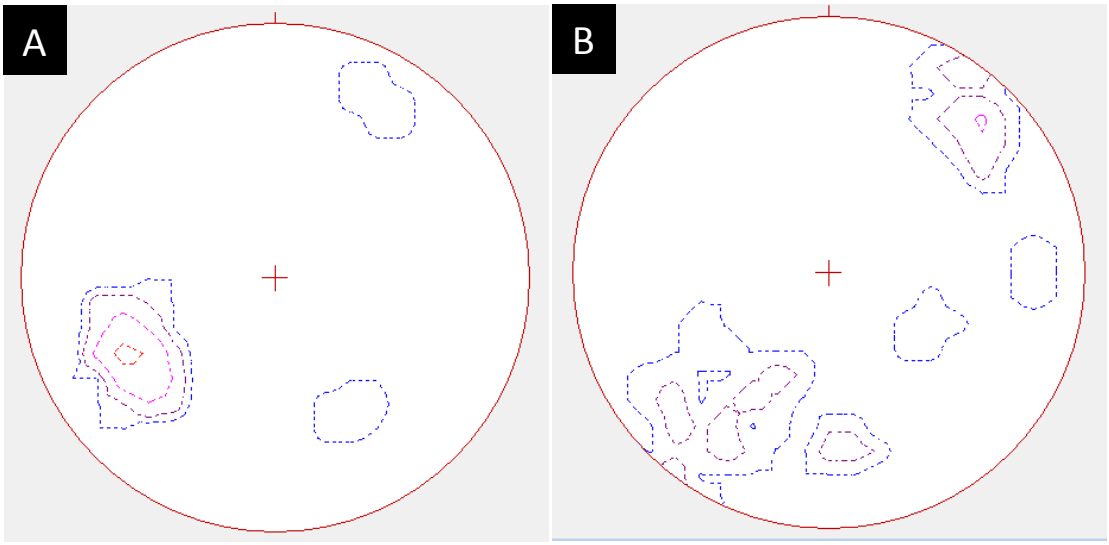

Figure 8.

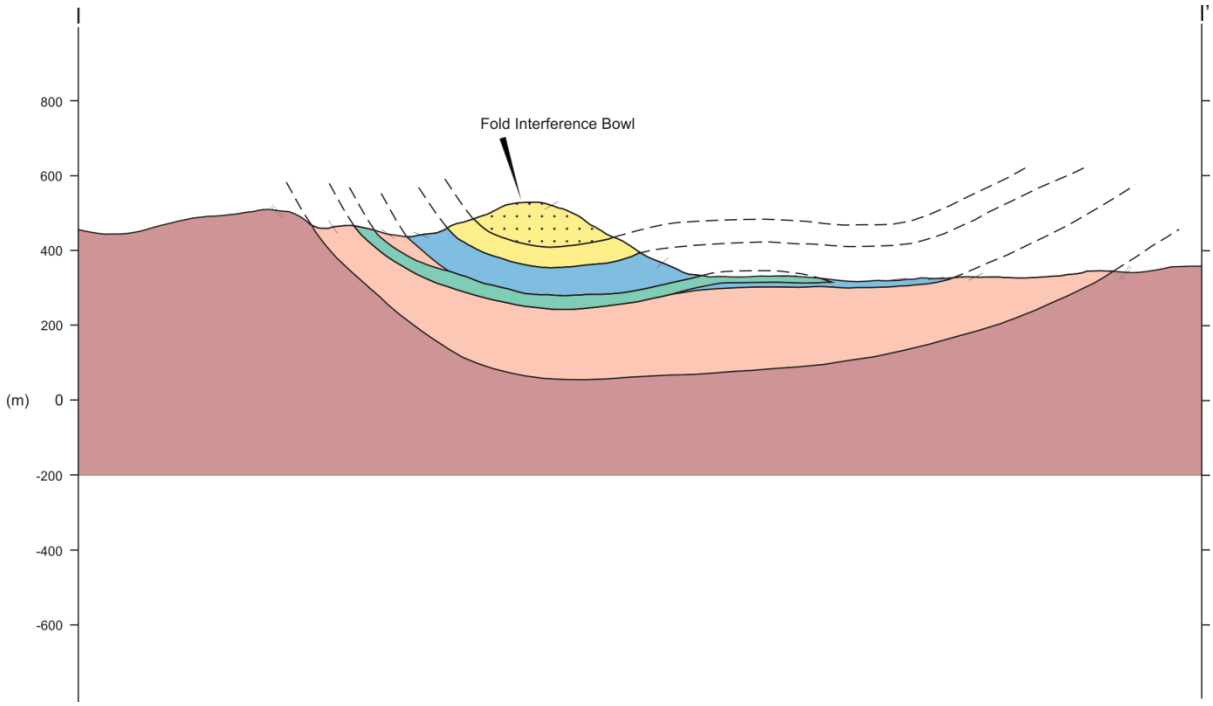

Figure 9.

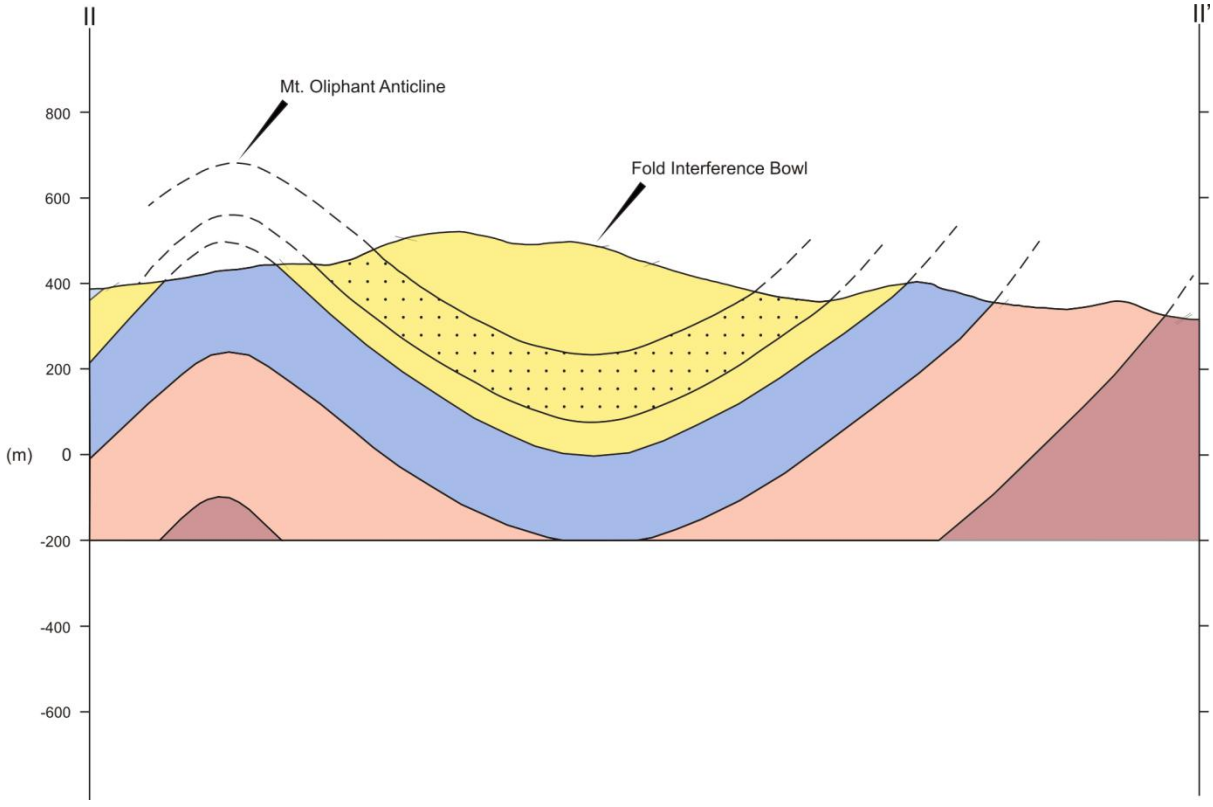

Figure 10.

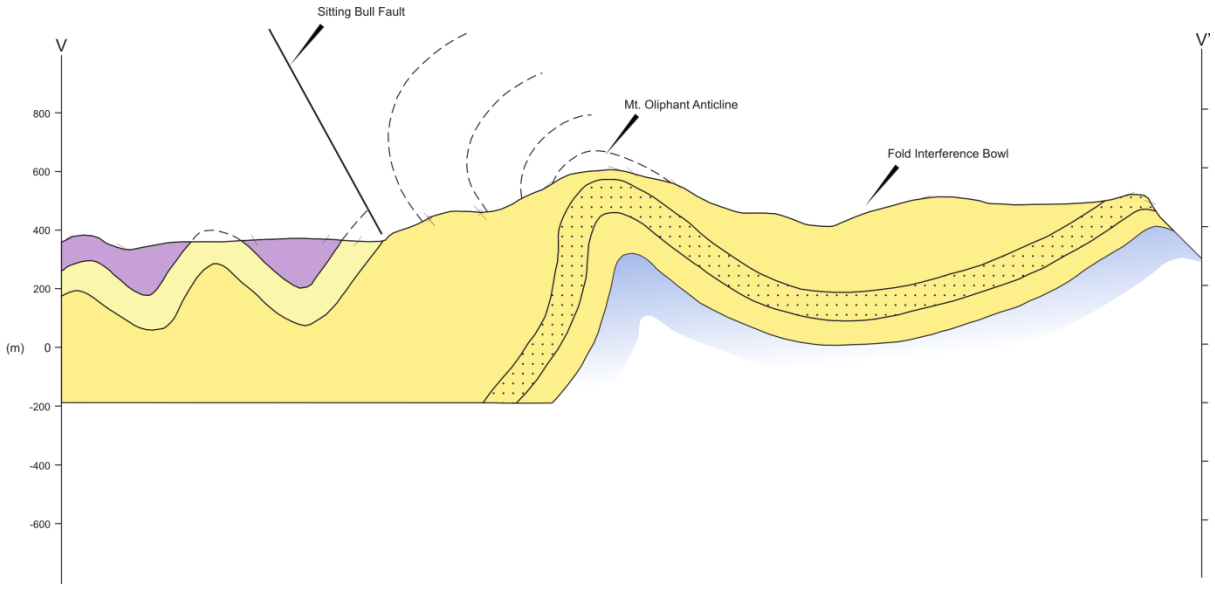

Figure 11.

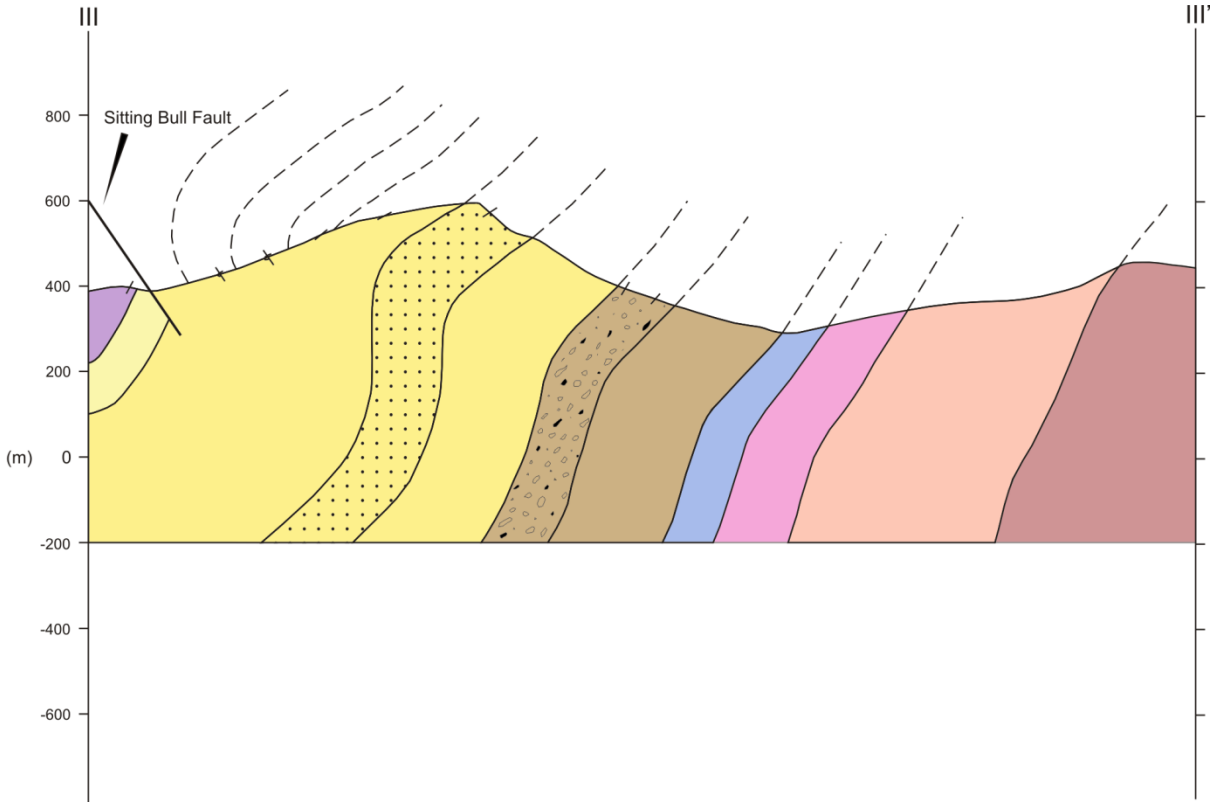

Figure 12.

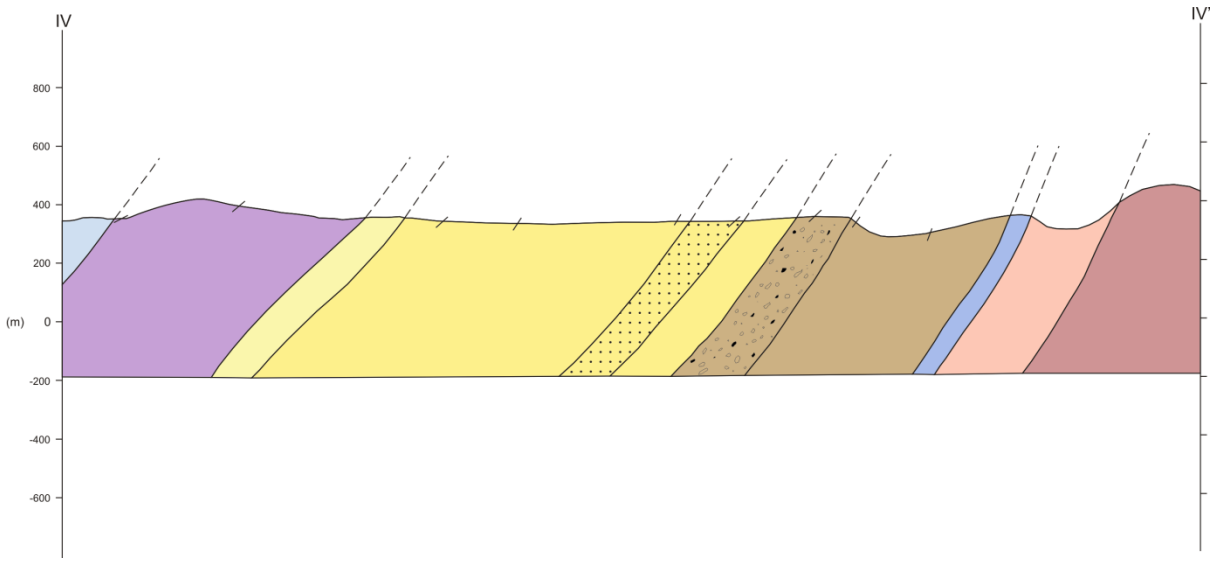

Figure 13.

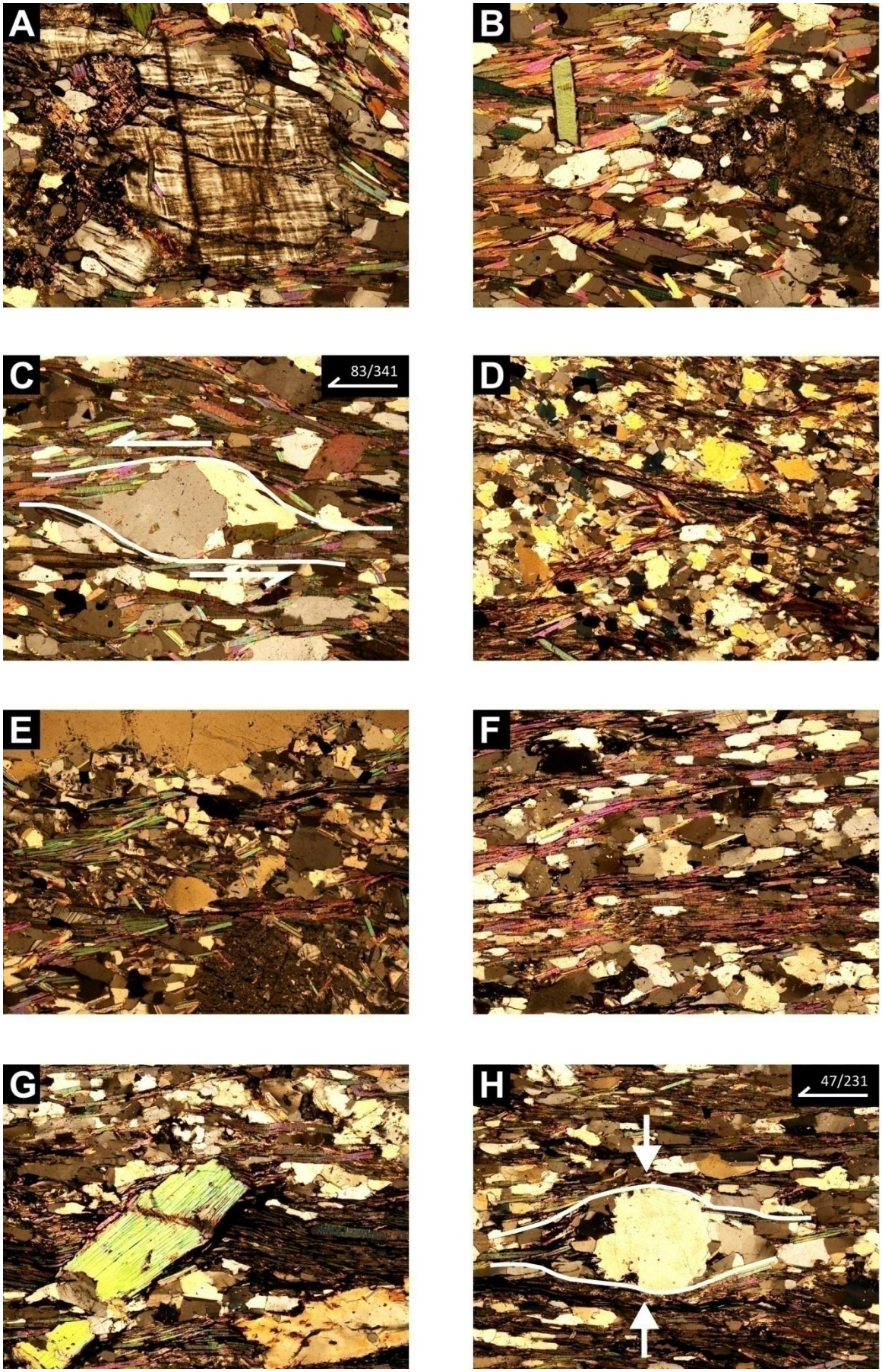

Figure 14.

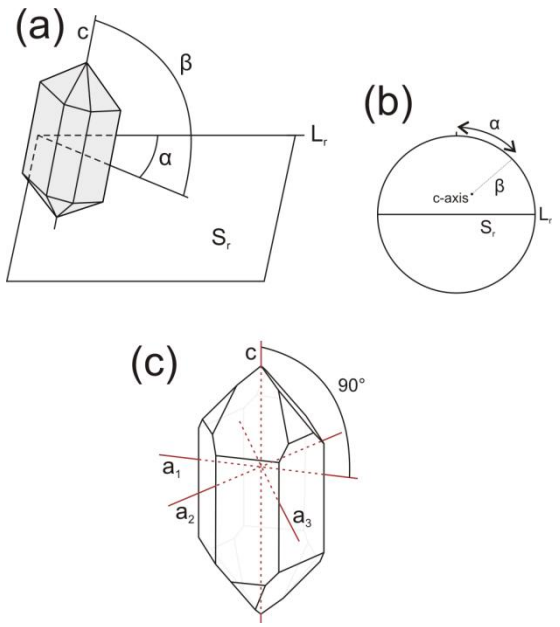

Figure 15

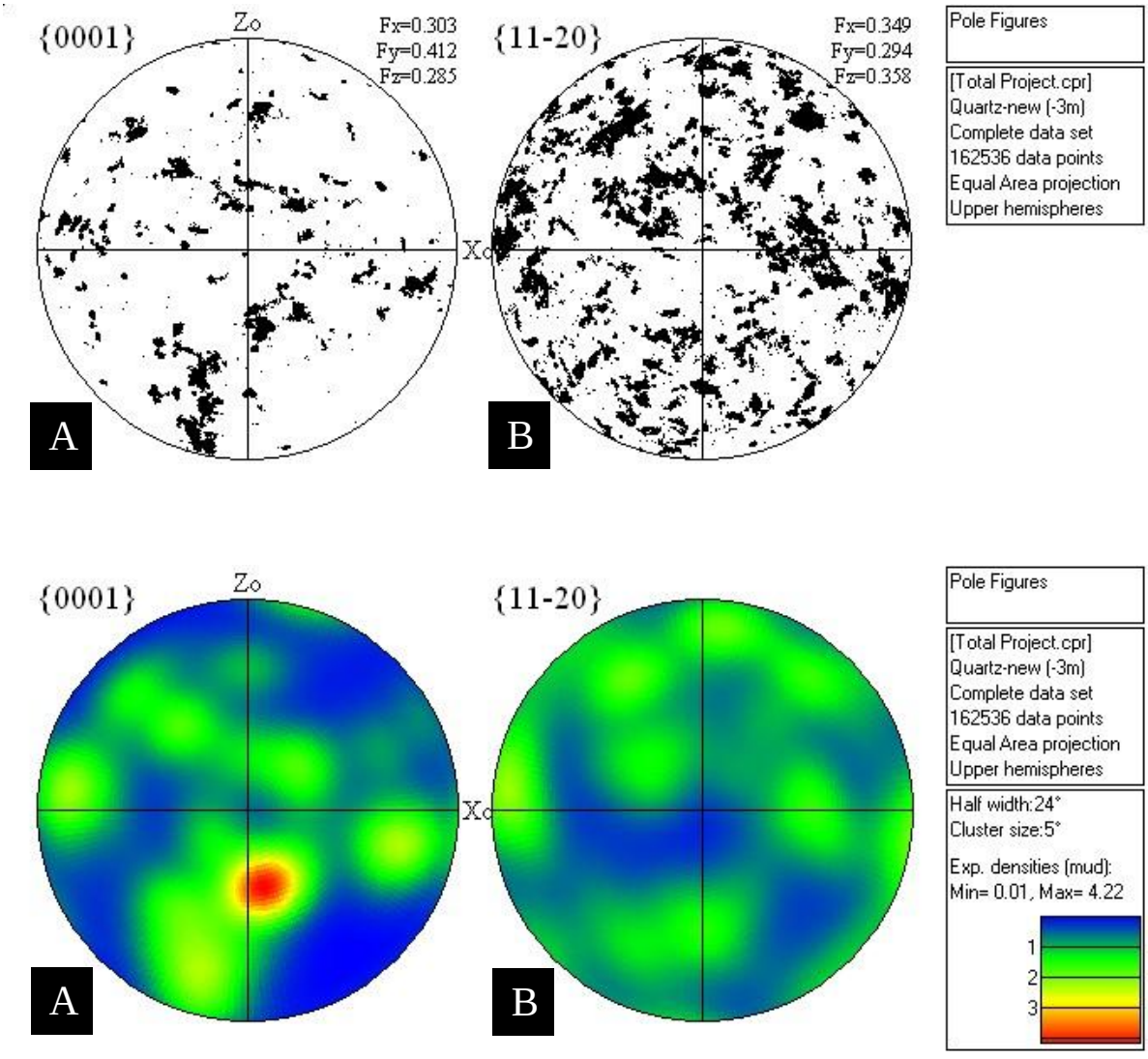

Figure 16.

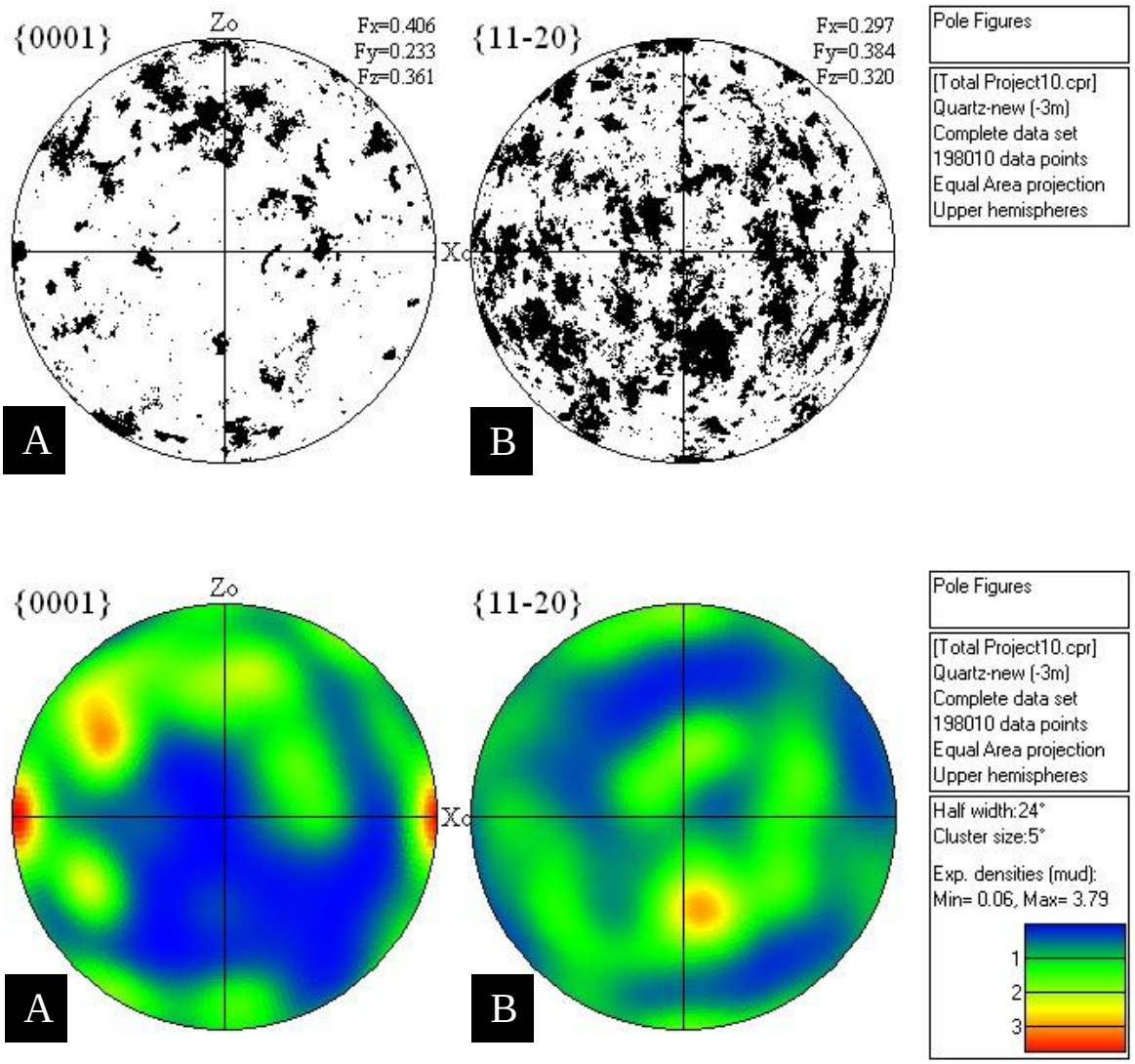
{0001}
Zo
Fx=0.406
Fy=0.233
Fz=0.361
Xo
{11-20}
Fx=0.297
Fy=0.384
Fz=0.320
Pole Figures
[Total Project10.cpr]
Quartz-new (-3m)
Complete data set
198010 data points
Equal Area projection
Upper hemispheres
A
B
{0001}
Zo
{11-20}
Xo
Pole Figures
[Total Project10.cpr]
Quartz-new (-3m)
Complete data set
198010 data points
Equal Area projection
Upper hemispheres
Half width:24°
Cluster size:5°
Exp. densities (mud):
Min= 0.06, Max= 3.79
1
2
3
A
B

Figure 17.

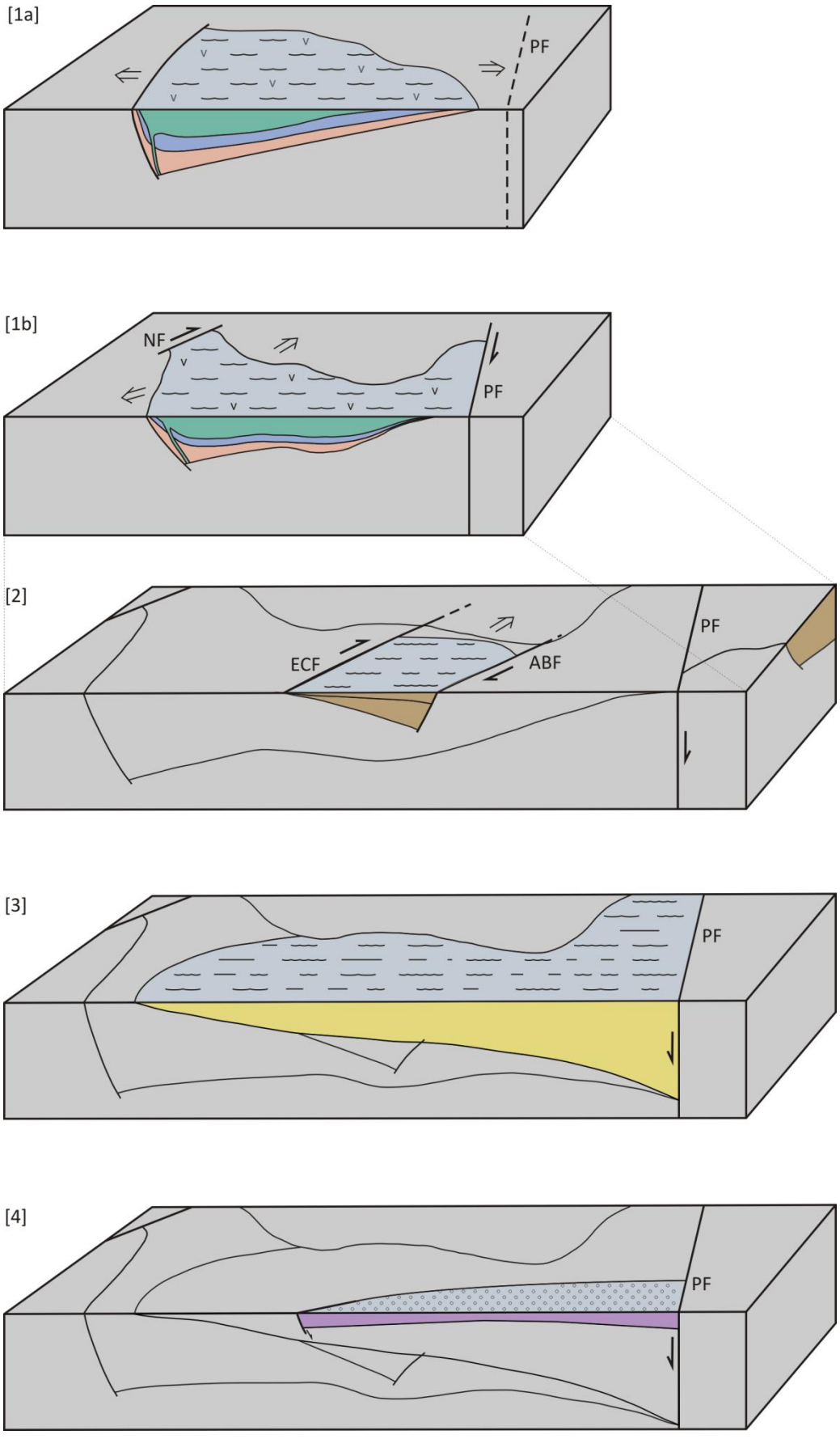
[1a]
PF
[1b]
NF
PF
[2]
ECF
ABF
PF
[3]
PF
[4]
PF

Figure 18.

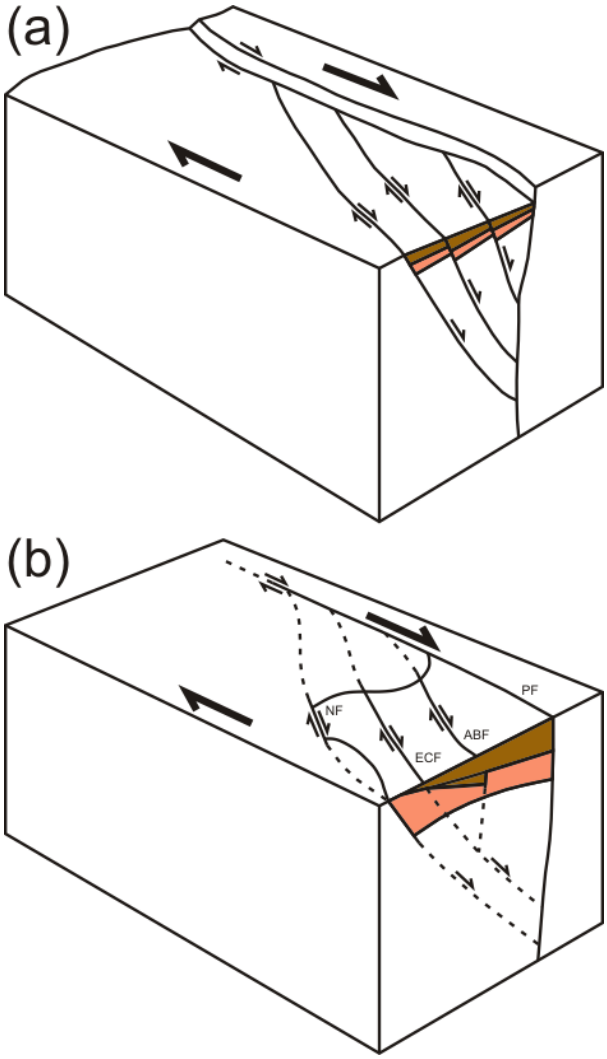

Figure 19.

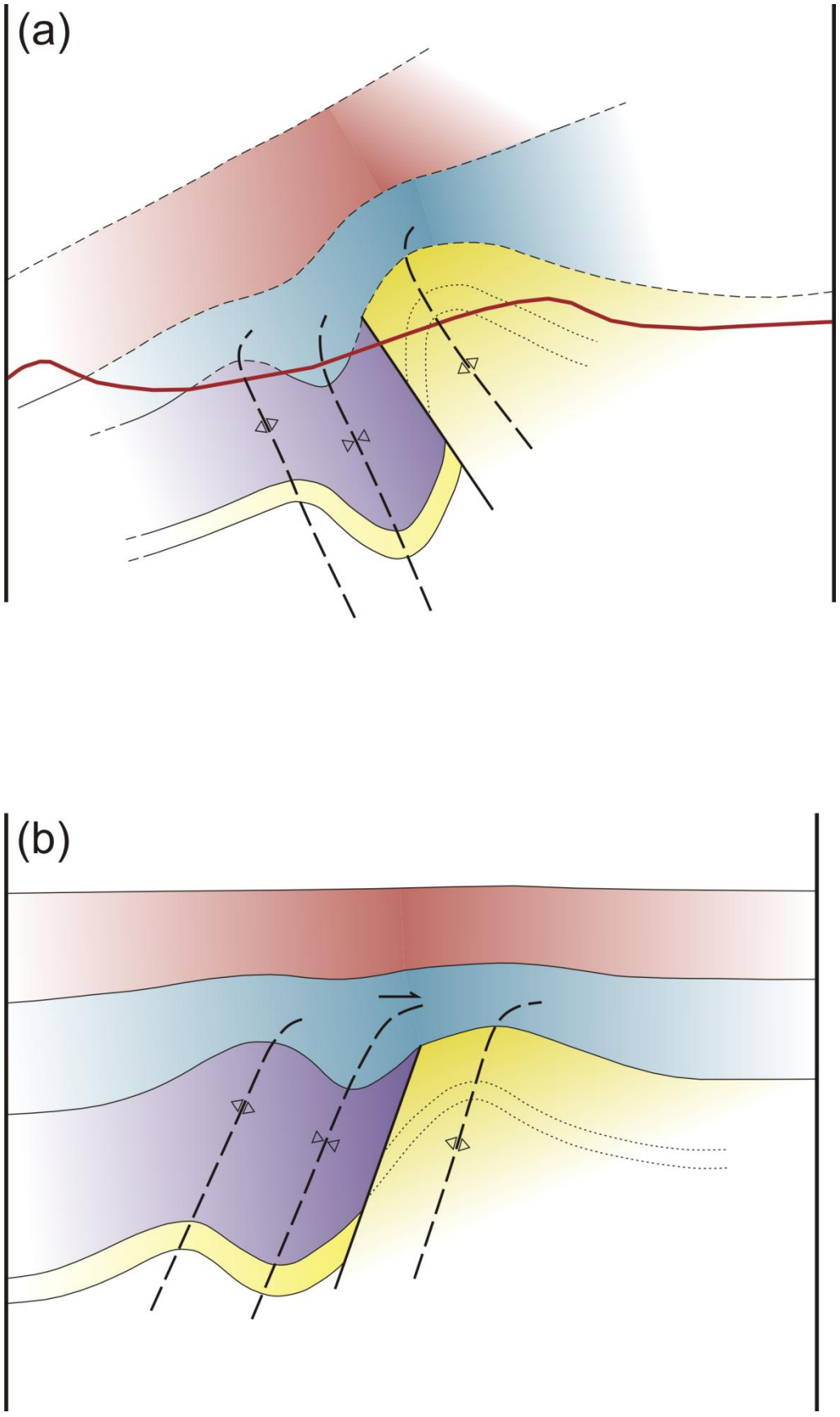

N

500 m

RAK1101

Arkaroola Creek

I'

II'

III'

IV'

V'

I

II

III

IV

V

MT PAINTER INLIER

RAK1110

RAK1107

ARKAROOLA WATERHOLE

ARKAROOLA PEGMATITE

RAK1103

Arkaroola Creek

Wywyana Creek

MT OLIPHANT

THE PINNACLES

SITTING BULL

ARKAROOLA VILLAGE

b

NF

ECF

ABF

KEY

- Lithological boundary
- Unconformable lithological boundary
- Inferred lithological boundary
- Synclinal axial trace
- Anticlinal axial trace
- Fault
- Inferred fault
- Bedding
- Overturned Bedding
- S_z foliation
- L_z lineation
- Fold plunge

LEGEND

PALAEOZOIC

ORDOVICIAN INTRUSIVES

PEGMATITIC INTRUSIVES: coarsely crystalline sodic leucogranites and granitic pegmatites.

NEOPROTEROZOIC

ADELAIDEAN

TORRENSIAN

MIDDLE BURRA GROUP

OPAMINDA FORMATION: Fine-grained green, actinolitic shales, dolomites and interbeds of dark grey silts and fine sands preserving mudcracks and ripple marks.

WILLOURAN

IDNYER BURRA GROUP

BLUE MINE CONGLOMERATE: Medium-grained, arkosic conglomerate with occasional heavy mineral laminations and cross-stratification. Heterogeneous, coarse sand-cobble size, sub-rounded clasts derived from underlying lithologies. Transitional package of gritty, clast poor micaceous arenite in underlying sedimentary contact.

WOODNAMOKA FORMATION: Highly variable meta-sedimentary unit of well laminated silty phyllites, biotite-andalusite-schists, medium-grained sandstones and micaceous arenites. Variable metamorphic grade with coarse, low-grade units displaying heavy mineral laminations and cross-stratification.

OLIPHANT ARKOSE MEMBER: Sub-basal member of medium- to coarse-grained pink-red weathering arkosic sandstone. Extensive heavy mineral laminations and cross-stratification.

ARKAROOLA CREEK BRECCIA MEMBER: Polymictic sedimentary breccia; pebble-cobble size clasts with a medium grained, quartzose, sandstone matrix.

HUMANITY SEAT FORMATION: Medium-grained, heavy mineral laminated meta-sandstone with interbedded massive quartzites and purple-grey shales. Extensive cross-stratification, scour & fills and ripple marks.

CALLANNA GROUP

WOOLTANA VOLCANICS: Grey-green to red-purple weathering basalts with porphyroblastic, vesicular and amygdaloidal textures in flows with minor meta-sedimentary interbeds. Abundance of metasomatic actinolite and epidote with minor anhydrite and tremolite.

WYWYWANA FORMATION: Actinolitic marbles, minor calc-silicate rocks and meta-siltstones. Fault related metasomatism to massive, actinolite rubbles.

PARALANA QUARTZITE: Medium-grained, massive, pink to grey weathering orthoquartzites, with argillaceous interbeds. Rare ripple marks and heavy mineral laminations. Basal sub-unit of poorly-sorted, grey-red weathering arkosic arenite. Fine sericite-kaolinite matrix between coarse, predominantly felspathic grit.

MESOPROTEROZOIC

CARPENTARIAN

MT PAINTER COMPLEX

MOUNT NEIL GRANITE PORHYRY: Granite porphyry with phenocrysts of blue-quartz. Locally mylonotised at contact with Adelaidean cover sequence.